EELS: recent developments and new perspectives

Cécile Hébert
Centre Interdisciplinaire de Microscopie Electronique
Laboratoire de Spectrométrie et Microscopie Electronique
Ecole Polytechnique Fédérale de Lausanne

EELS in the TEM: recent developments and new perspectives

Cécile Hébert
Centre Interdisciplinaire de Microscopie Electronique
Laboratoire de Spectrométrie et Microscopie Electronique
Ecole Polytechnique Fédérale de Lausanne

Outline

- Introduction: EELS in the TEM
- Core losses
- Low losses
- Even lower losses
- Conclusion

Outline

- Introduction: EELS in the TEM
- Core losses
- Low losses
- Even lower losses
- Conclusion

EWinS2016

The constituent of the TEM

A typical TEM: Jeol 200cx

Probe = electrons
100-300 kV
Velocity: 0.55-0.77 c

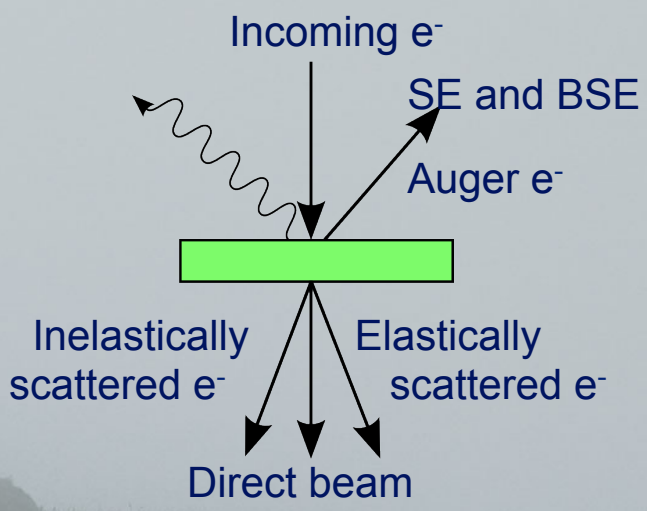

The objective lens

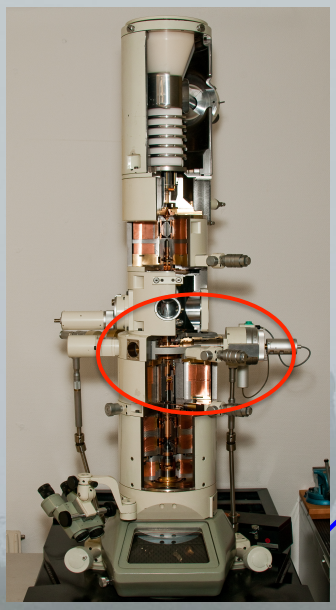

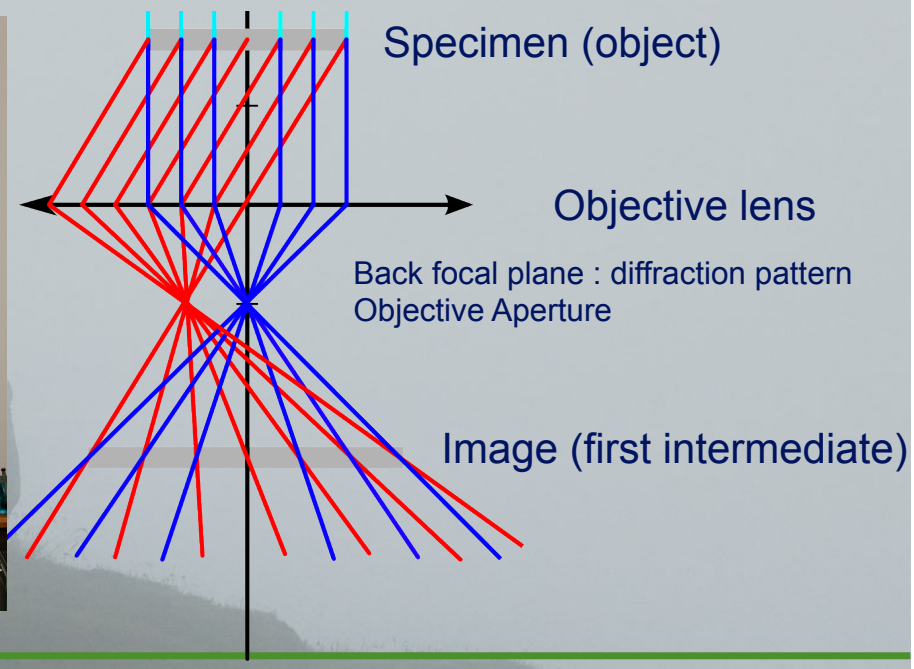

Diffraction theory - Bragg law

Path difference between reflection from planes distance d_{hkl} apart = $2d_{hkl}\sin\theta$

$2d_{hkl}\sin\theta = \lambda$ - constructive interference

=> Bragg law: $n\lambda = 2d_{hkl}\sin\theta$

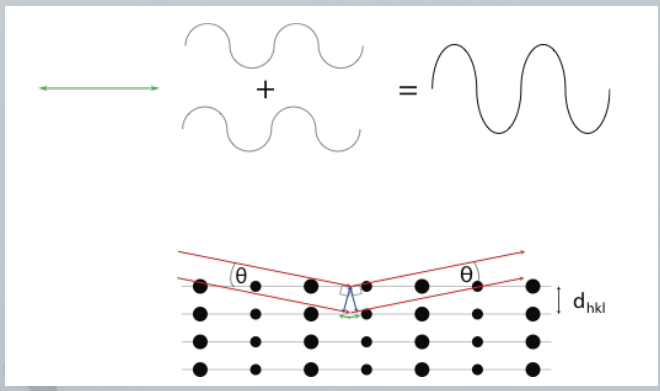

Electron diffraction: $\lambda \sim 0.001$ nm therefore: $\lambda \ll d_{hk}$

=> small angle approximation: $n\lambda \approx 2d_{hkl}\theta$

@ 200 kV λ~2.5pm; d~0.25nm -> 2θ~10mrad

Reciprocity: scattering angle $\theta \propto d_{hkl}^{-1}$

STEM & STEM-EELS

- The electron beam is formed as as **focused probe** scanned on the sample
- The signal is acquired on the detectors pixel by pixel
- The focused probe is a convergent electron beam. The bright field and Dark field detectors are radially symmetric
- The convergence semi-angle of the probe is called α. Typicall 10-30 mrad
- EELS is acquired in the hole of the DF detector (retracting the BF one). Collection angle is <= convergence in general.

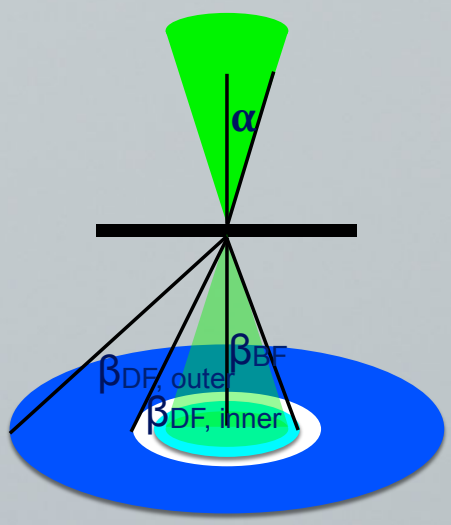

Instrumentation

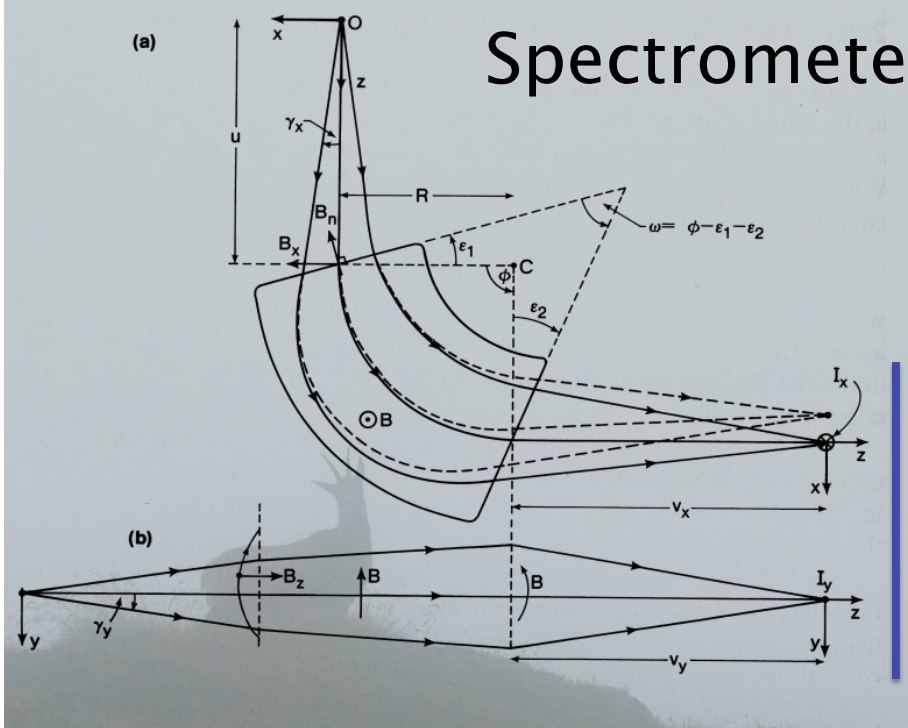

Excitation process for EELS

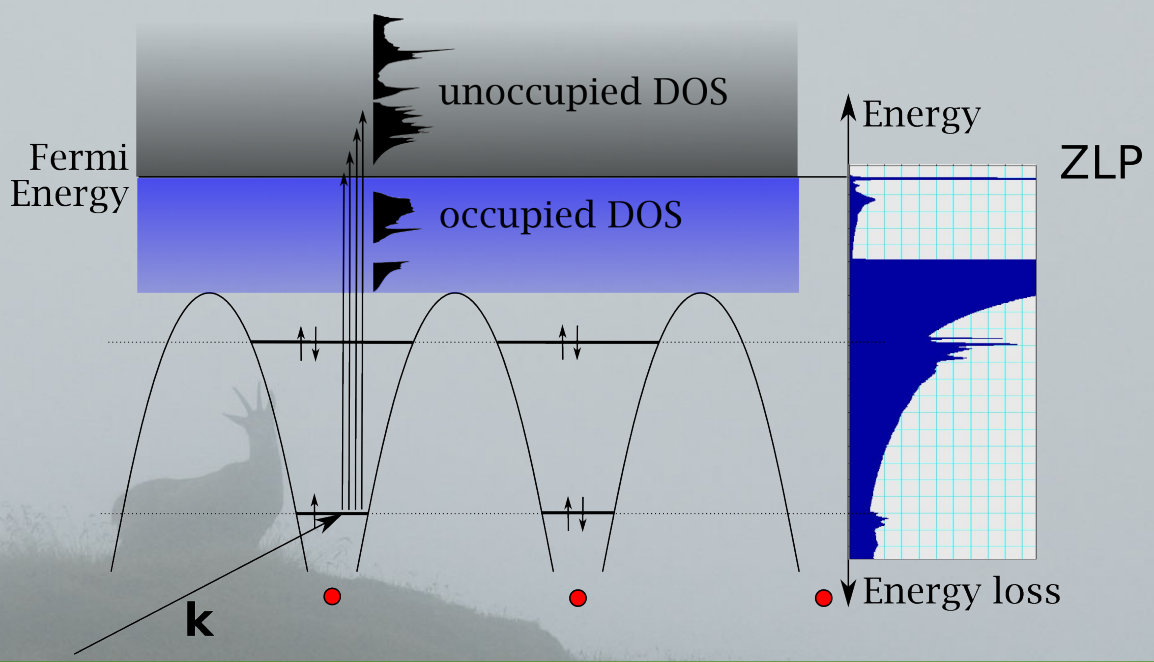

Accesible data range

E_0=100-300kV

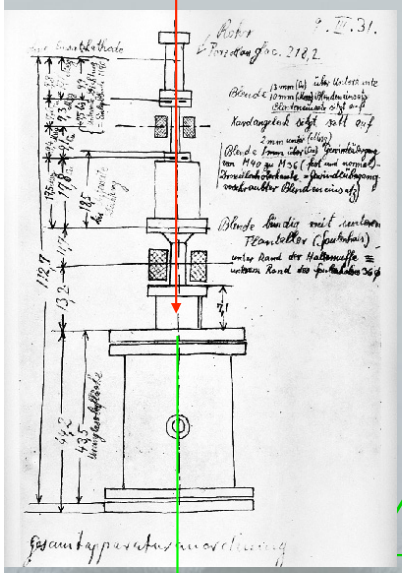

ΔE=0-3kV

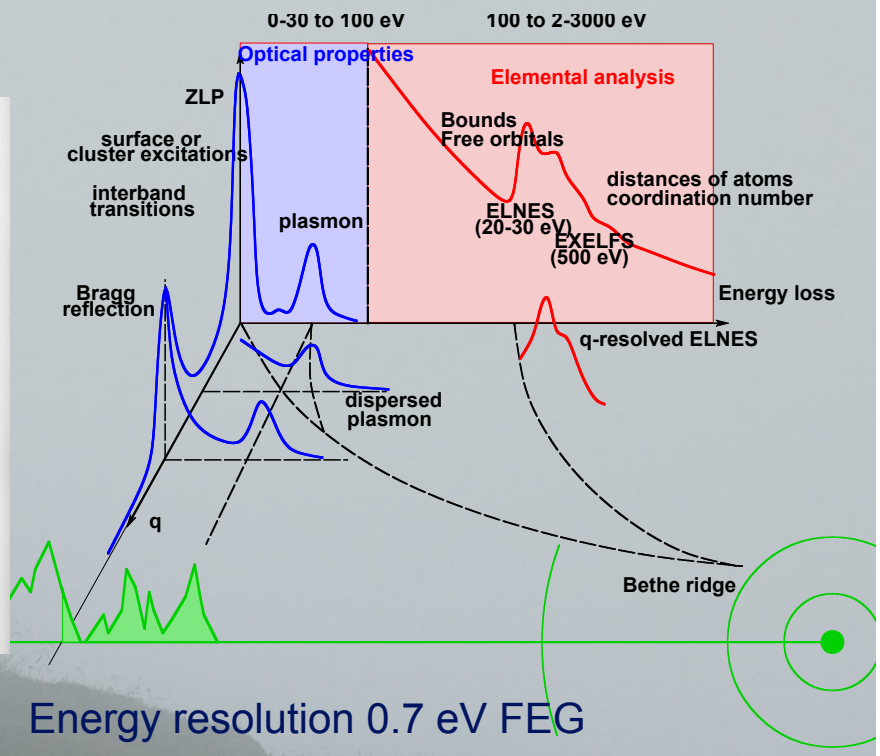

Energy resolution 0.7 eV FEG

Scattering geometry

Scattering geometry

$$q^2 = k^2 + (k')^2 - 2kk'\cos\theta$$

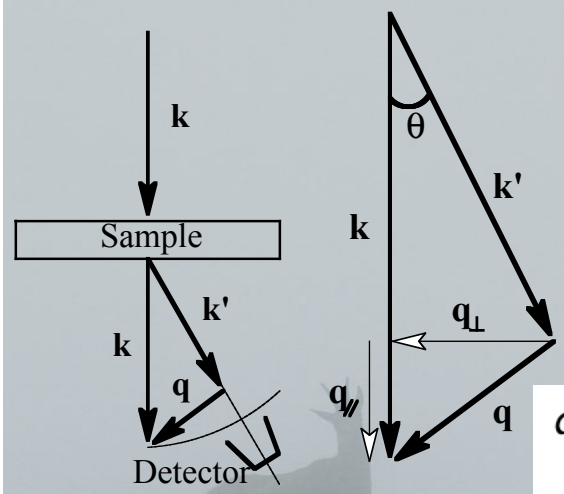

0 < θ < 100 mrad

To avoid aberrations
0 < θ < 25 mrad

@200 kV [111] spot
in fcc Cu: 11 mrad

$$q_\perp = k\vartheta \text{ (geometry)}$$

$$q_\parallel = k\vartheta_E \text{ (definition of } \vartheta_E)$$

$$\vartheta \ll 1 \text{ therefore } q^2 = k^2(\vartheta_E^2 + \vartheta^2)$$

$$\theta_E = \Delta E m\gamma/\hbar^2 k^2$$

Outline

- Introduction: EELS in the TEM
- Core losses
- Low losses
- Even lower losses
- Conclusion

Core losses

Core losses

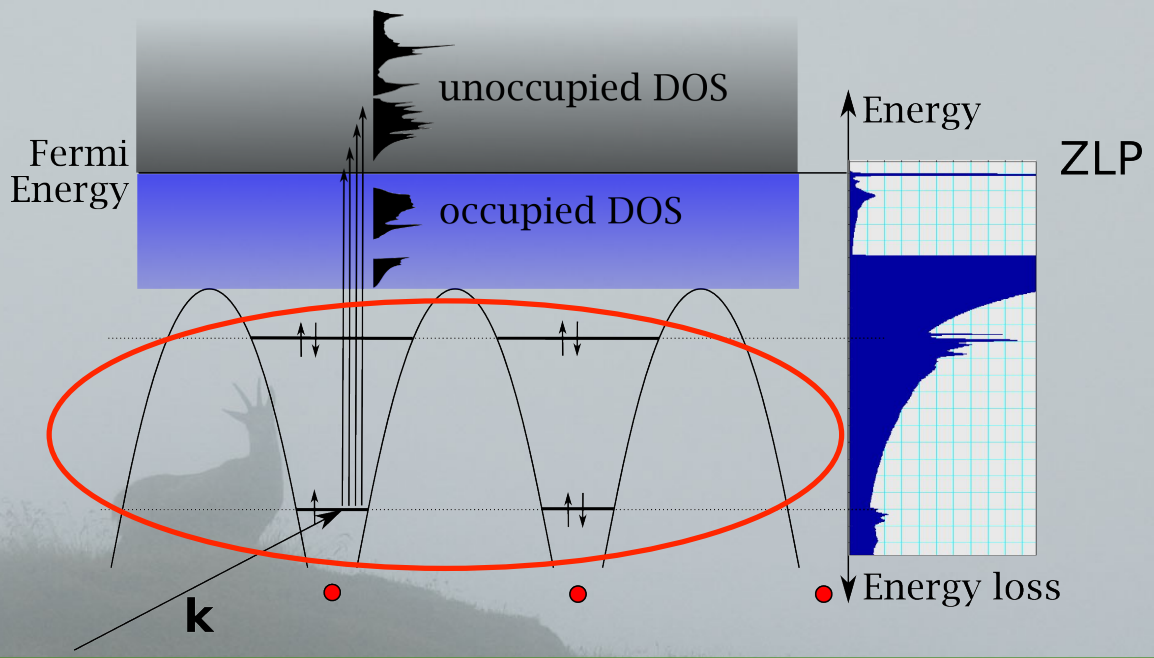

Core losses

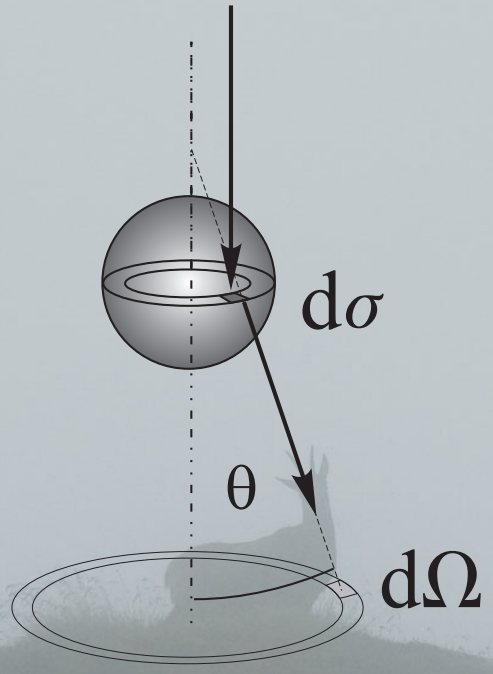

Relevant quantity: scattering cross-section as a function of angle q and energy loss E.

It is given for one atom.

We consider a transition from initial state | I > to final state | F > for the core electron of the atom

q: momentum transfer

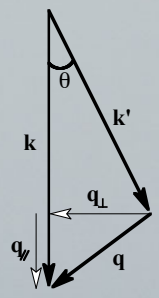

Theory of core losses

transition from core (occupied) to unoccupied state
We need quantum mechanics!
System = fast incoming electron + target electron
first order perturbation theory
First Born approximation
perturbation potential is Coulomb potential

H.A.Bethe: 1930:

Zur Theorie des Durchgangs schneller Korpuskularstrahlen durch Materie

Annalen der Physik, vol. 397, Issue 3, pp.325-400

Theory of core loss

Transition probability per unit time dP_{if} from an initial state $|i\rangle$ to a final state $|f\rangle$ situated between ν_f and $\nu_f + d\nu_f$.

$$dP_{if} = \frac{2\pi}{\hbar}|\langle f|V|i\rangle|^2 d\nu_f\, \delta(E_i - E_f)$$

Initial and final state of the system :

$$\begin{aligned} |i\rangle &= |\vec{k}\rangle \otimes |I\rangle \\ &\textit{and} \\ |f\rangle &= |\vec{k}'\rangle \otimes |F\rangle \end{aligned}$$

$|I\rangle$ and $|F\rangle$ Initial and final states of the target electron.

Theory of core loss

$\vec{k}$ before the interaction $\vec{k}'$ after.

$\vec{q} = \vec{k} - \vec{k}'$

$$dP_{if} = \frac{2\pi}{\hbar}\left|\langle F| \otimes \langle \vec{k}'|V|\vec{k}\rangle \otimes |I\rangle\right|^2 d\nu_f \delta(E_I - E_F + E)$$

$\langle \vec{k}'|V|\vec{k}\rangle$? ? $\longrightarrow$ V Coulomb potential

$$\langle \vec{k}'|V|\vec{k}\rangle = \frac{1}{4\pi\epsilon_0}\int (2\pi)^{-3} d^3r \frac{e^2}{|\vec{r} - \vec{R}|} e^{i(\vec{k}-\vec{k}')\vec{R}}$$

$\vec{r}$ position vector of the fast electron $\vec{R}$ of the target electron

Theory of core loss

$$\langle \vec{k}' | V | \vec{k} \rangle = \frac{e^2}{(2\pi)^3 \epsilon_0 q^2} e^{i\vec{q}.\vec{R}}$$

$$dP_{if} = \frac{e^4}{(2\pi)^5 \hbar \epsilon_0^2 q^4} |\langle F | e^{i\vec{q}.\vec{R}} | I \rangle|^2 d\nu_f \, \delta(E_I - E_F + E)$$

Theory of core loss

$$d\sigma = \sum_{i,f} \frac{dP_{if}}{j_0}$$

j_0 current density of the plane wave

$\psi_{\vec{k}}(\vec{R}) = (2\pi)^{-3/2} e^{i\vec{k}.\vec{R}}$ $\qquad$ $j_0 = (\hbar k)/((2\pi)^3 m)$

$$d\sigma = \sum_{I,F} \frac{me^4}{(\hbar 2\pi \varepsilon_0)^2 q^4 k} |\langle F | e^{i\vec{q}.\vec{R}} | I \rangle|^2 d\nu_f \delta(E_I - E_F + E)$$

$d\nu_f = d\nu_t \, d\nu_e$ ($d\nu_t$: target electron, $d\nu_e$: fast electron)

$d\nu_e = (k'm)/\hbar^2 dE d\Omega$

Theory of core loss

If the final state is expressed in an orthogonal basis set :
$d\nu_t = 1$

$$d\nu_f = k' \frac{m}{\hbar^2} dE d\Omega$$

$$\frac{\partial^2 \sigma}{\partial E \partial \Omega} = \sum_{I,F} 4 \frac{m^2 e^4}{\hbar^4 (4\pi)^2 \varepsilon_0^2 q^4} \frac{k}{k'} |\langle F | e^{i\vec{q}.\vec{R}} | I \rangle|^2 \delta(E_I - E_F + E)$$

Relativistic effects : $m \rightarrow \gamma m$

Introduction

$$\frac{\partial^2 \sigma}{\partial E \partial \Omega} = \sum_{I,F} \frac{4\gamma^2}{a_0^2 q^4} \frac{k'}{k} |\langle F | e^{i\vec{q}.\vec{R}} | I \rangle|^2 \delta(E_I - E_F + E) = \frac{4\gamma^2}{a_0^2 q^4} \frac{k'}{k} S(\vec{q}, E)$$

$$S(\vec{q}, E) = \sum_F |\langle F | e^{i\vec{q}.\vec{R}} | I \rangle|^2 \delta(E_I - E_F + E)$$

S: Dynamic form factor

a_0 : Bohr radius

$$a_0 = \frac{4\pi\varepsilon_0 \hbar^2}{me^2}$$

$\vec{q} = \vec{k} - \vec{k'}$

$\gamma = (1 - v^2/c^2)^{-1/2}$

R F Egerton, *Electron energy-loss spectroscopy in the TEM*, Rep. Prog. Phys. 72 (2009) 016502 (25pp); Egerton R F 1996 *Electron Energy-Loss Spectroscopy in the Electron Microscope* 2nd edn (New York: Plenum/Springer)

Introduction

$$S(\vec{q},E) = \sum_F |\langle F|e^{i\vec{q}.\vec{R}}|I\rangle|^2 \delta(E_I - E_F + E)$$

Final state: ??

Initial state:
Core state

Easiest approximation: forget about crystal: atomic model (Hydrogenic, Hartree –Slater, …)

Used for quantification. Can already explain some features

Next step: take crystal into account for |F>

Further : consider real electron wave in the crystal (instead of plane wave) e.g. P. Schattschneider, Oxley & Pantelides

Introduction

Dipole approximation

$$S(\vec{q},E) = \sum_F |\langle F|e^{i\vec{q}.\vec{R}}|I\rangle|^2 \delta(E_I - E_F + E)$$

If $\vec{q}.\vec{R} \ll 1$ we can write $e^{i\vec{q}.\vec{R}} \simeq 1 + i\vec{q}.\vec{R}$

$$S(\vec{q},E) = \sum_F |\langle F|i\vec{q}.\vec{R}|I\rangle|^2 \delta(E_I - E_F + E)$$

$$S(\vec{q},E) \propto q^2 \quad ; \quad \frac{\partial^2\sigma}{\partial E \partial\Omega} \propto \frac{1}{q^4} S(\vec{q},E)$$

with the scattering geometry, $q^2 = k^2(\vartheta_E^2 + \vartheta^2)$

Lorenzian distribution $\boxed{\frac{\partial^2\sigma}{\partial E \partial\Omega} \propto \frac{1}{\vartheta^2 + \vartheta_e^2}}$

Core loss EELS: theory

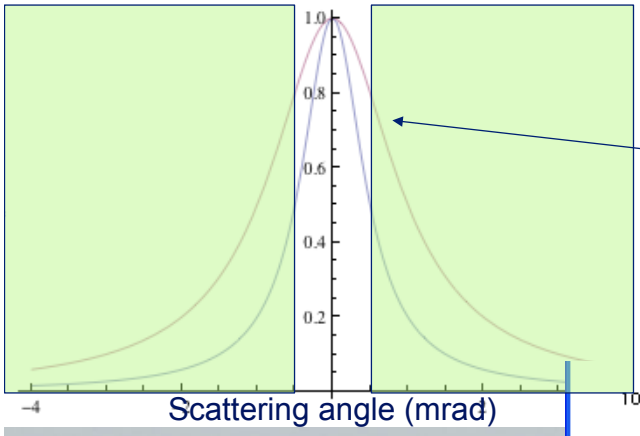

Cutoff (obj. aperture)

Example BN
B-K @200 eV
N-K @400 eV

$$\theta_E = \Delta E m\gamma/\hbar^2 k^2$$

$\theta_E \sim \Delta E/2E_0$; @200kV:

$\theta_{E\ B\text{-}K}$=0.5 mrad
$\theta_{E\ N\text{-}K}$=1 mrad

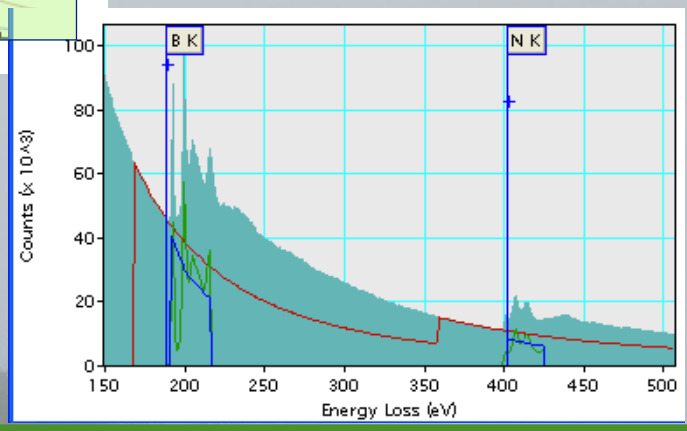

$$S(\vec{q}, E) = \sum_F |\langle F|e^{i\vec{q}.\vec{R}}|I\rangle|^2 \delta(E_I - E_F + E)$$

Final state: ??

Initial state:
Core state

Easiest approximation: forget about crystal: atomic model

- **Orientation dependence of the EELS of graphitic material**
- White lines and their applications

ELNES: Introduction

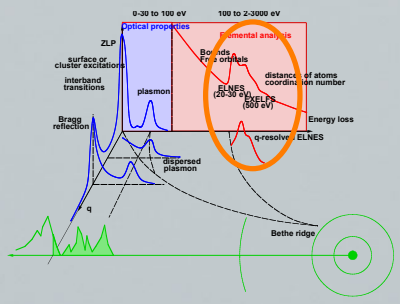

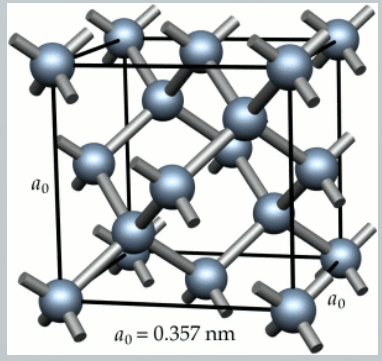

Diamond

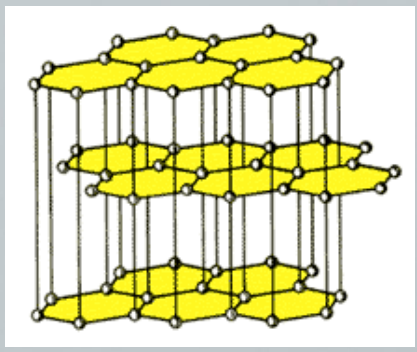

Graphite

Carbon K edge

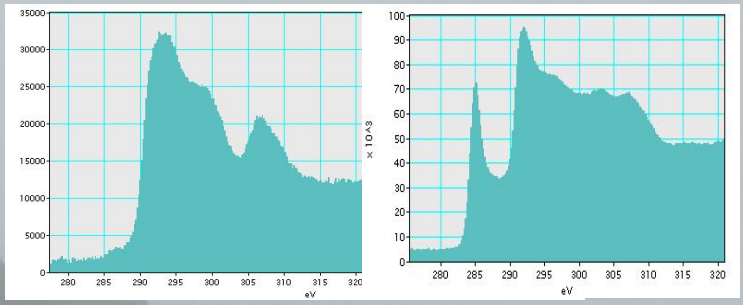

ELNES: anisotropy

ELNES of anisotropic materials

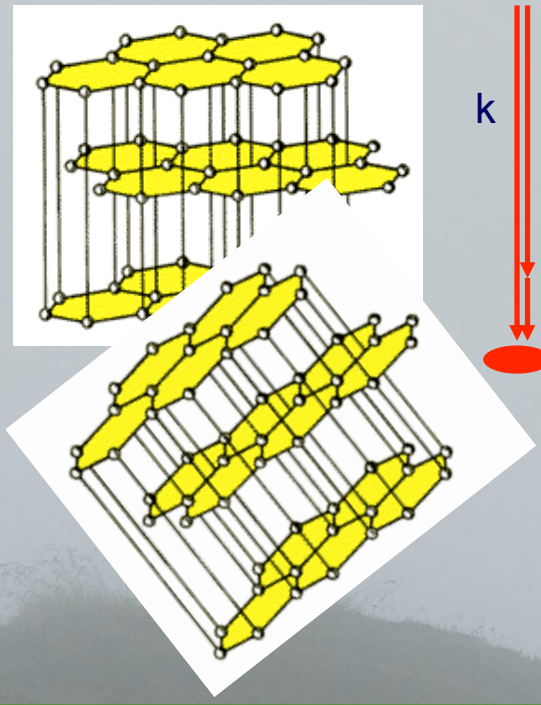

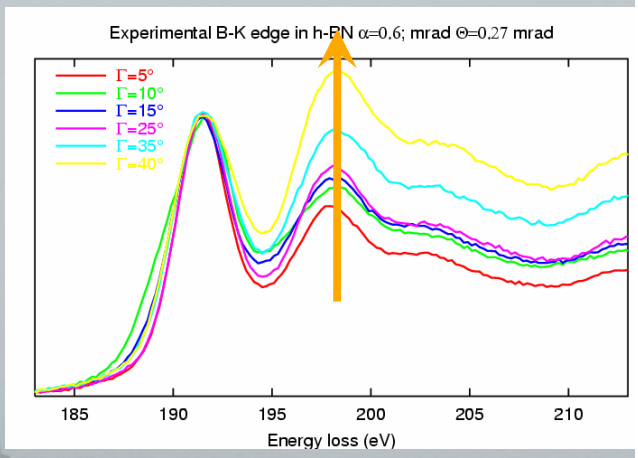

ELNES: anisotropy

ELNES of anisotropic materials

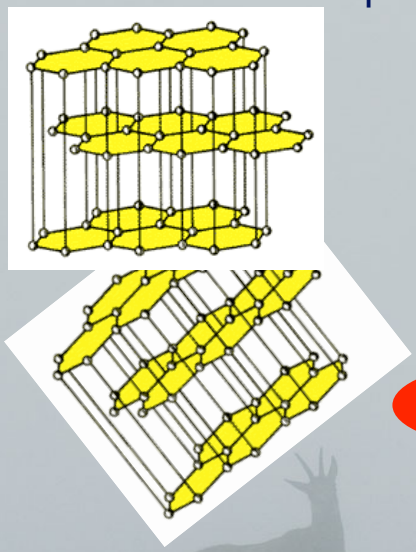

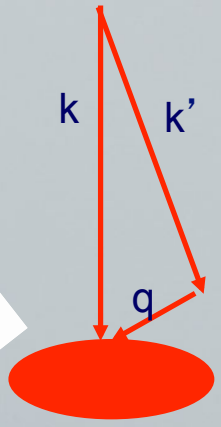

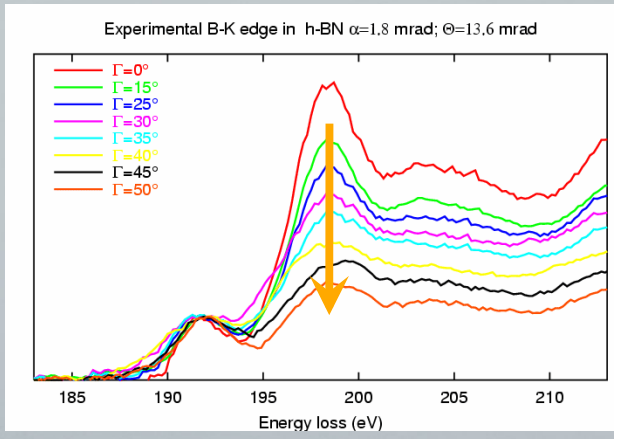

ELNES: anisotropy/relativity

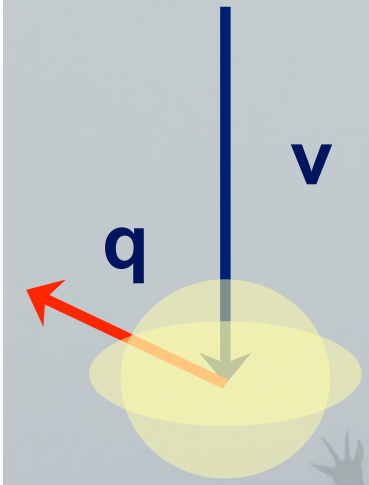

Electric field of a moving charge is compressed in the direction of movement

Coulomb coupling becomes anisotropic

Coupling with momentum transfer parallel to the electron's trajectory becomes smalle

Coupling with momentum transfers perpendicular to the electron's trajectory becomes larger

P. Schattschneider, C. Hébert, H. Franco, and B. Jouffrey. PRB, 72:045142–1 – 045142–8, 2005.
Hébert & al. Ultramicroscopy 106 (2006) 1139

ELNES: anisotropy

Magic angle conditions

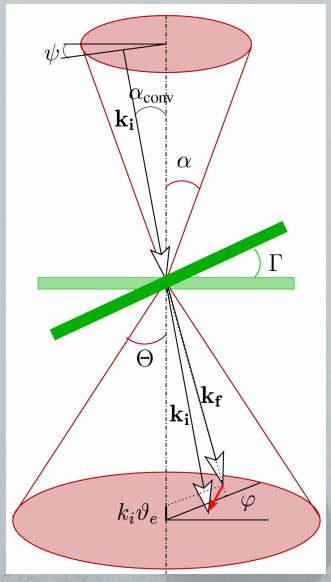

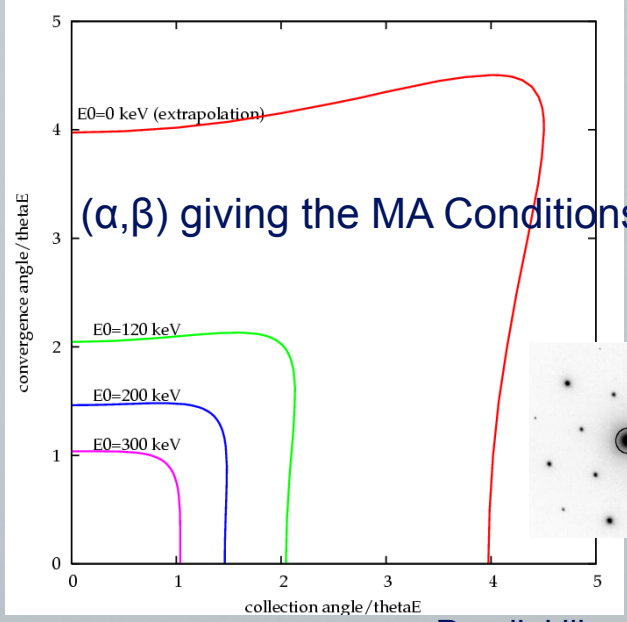

(α,β) giving the MA Conditions

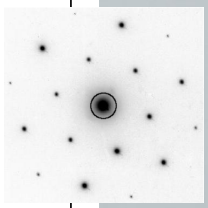

Hébert & al. Ultramicroscopy 106 (2006) 1139

Parallel illumination
Work in diffraction
Choose right cam length/collection angle

ELNES: anisotropy

Sample: graphite
[001] orientation

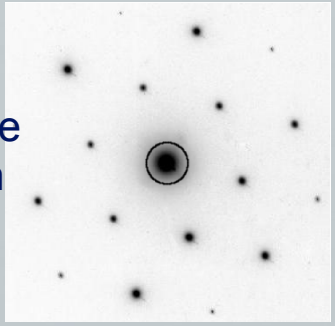

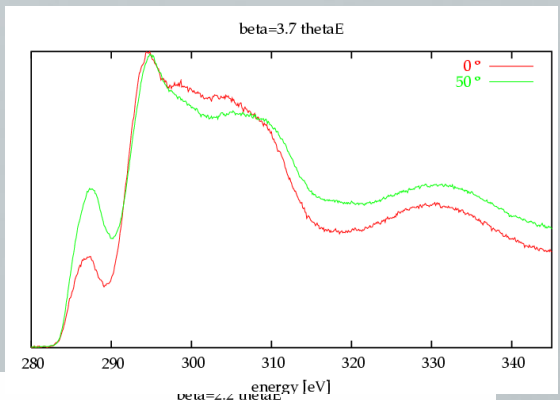

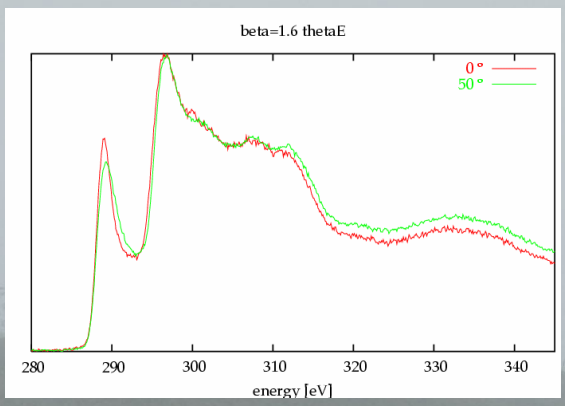

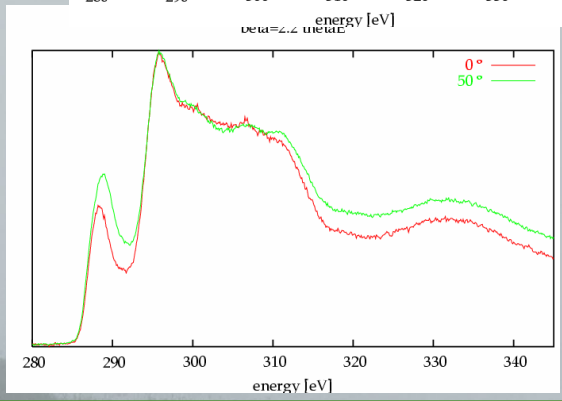

Application: sp2/sp3 ratio

Nanocarbon as Robust Catalyst: Mechanistic Insight into Carbon-Mediated Catalysis**

Jian Zhang, Dangsheng Su, Aihua Zhang, Di Wang, Robert Schlögl, and Cécile Hébert*

Angew. Chem. Int. Ed. **2007**, *46*, 1–6

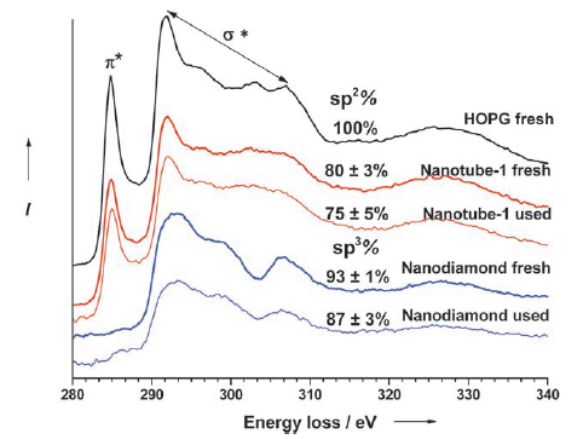

Figure 4. ELNES spectra of fresh and used nanocarbons.

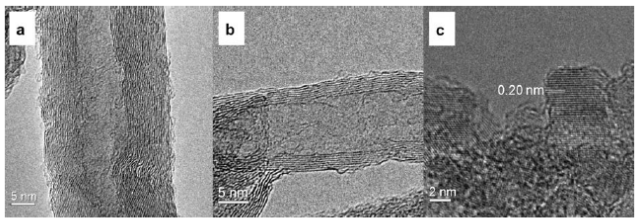

Figure 3. HRTEM images of used nanocarbons: a) nanotube-1; b) nanotube-2; c) nanodiamond.

Relativistic spectra Wien2k

- TELNES3 can calculate the DDSCS using any of three interaction potentials

- Nonrelativistic :

$$\frac{\partial^2\sigma}{\partial E\partial\Omega}=\left[\frac{4\gamma^2 a_0^{-2}}{q^2}\right]^2\frac{k_f}{k_i}\sum_{i,f}\left|\left\langle f\left|e^{i\boldsymbol{q}.\boldsymbol{r}}\right|i\right\rangle\right|^2\delta\left(E_f-E_i-E\right)$$

- Relativistic :

$$\frac{\partial^2\sigma}{\partial E\partial\Omega}=\left[\frac{4\gamma^2 a_0^{-2}}{q^2-\left(E/\hbar c\right)^2}\right]^2\frac{k_f}{k_i}\sum_{i,f}\left|\left\langle f\left|e^{i\boldsymbol{q}.\boldsymbol{r}}\left(1-\frac{\boldsymbol{v}_0.\boldsymbol{p}}{m_e c^2}\right)\right|i\right\rangle\right|^2\delta\left(E_f-E_i-E\right)$$

- Relativistic small q (dipole) approximation :

$$\frac{\partial^2\sigma}{\partial E\partial\Omega}=\left[\frac{4\gamma^2 a_0^{-2}}{q^2-\left(E/\hbar c\right)^2}\right]^2\frac{k_f}{k_i}\sum_{i,f}\left|\left\langle f\left|\tilde{\boldsymbol{q}}.\boldsymbol{r}\right|i\right\rangle\right|^2\delta\left(E_f-E_i-E\right)$$

P. Schattschneider, C. Hébert, H. Franco, and B. Jouffrey. PRB, 72:045142–1 – 045142–8, 2005.

Relativistic spectra Wien2k

Graphite C K for 3 tilt angles.
Beam energy 300 keV, collection angle = 2.4mrad.

Left: nonrelativistic calculation. Right: relativistic calculation.

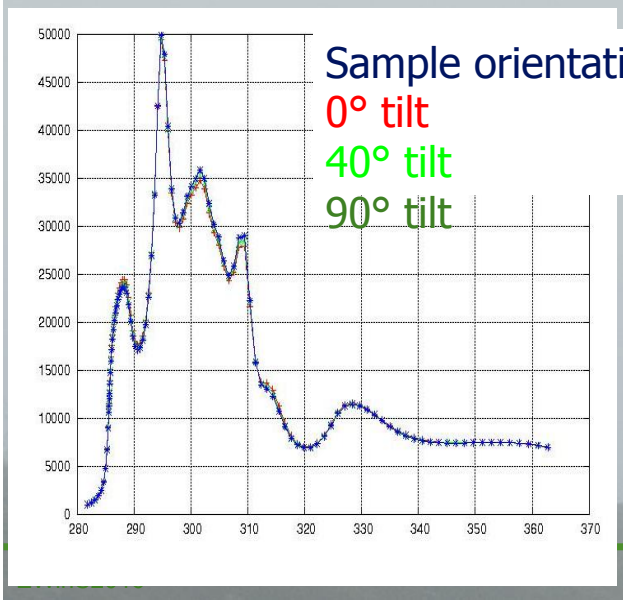

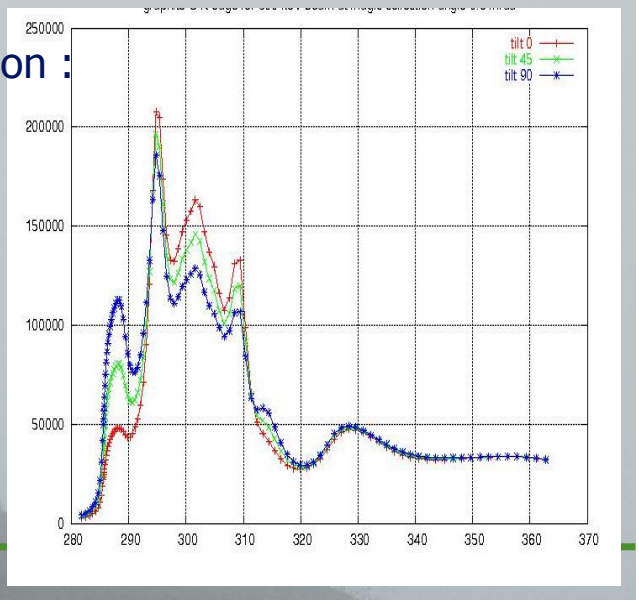

White lines

$$S(\vec{q}, E) = \sum_F |\langle F|e^{i\vec{q}.\vec{R}}|I\rangle|^2 \delta(E_I - E_F + E)$$

Final state: ??

Initial state:
Core state

Easiest approximation: forget about crystal: atomic model

- Orientation dependence of the EELS of graphitic material
- **White lines and their applications**

ELNES: fine structure interpretation

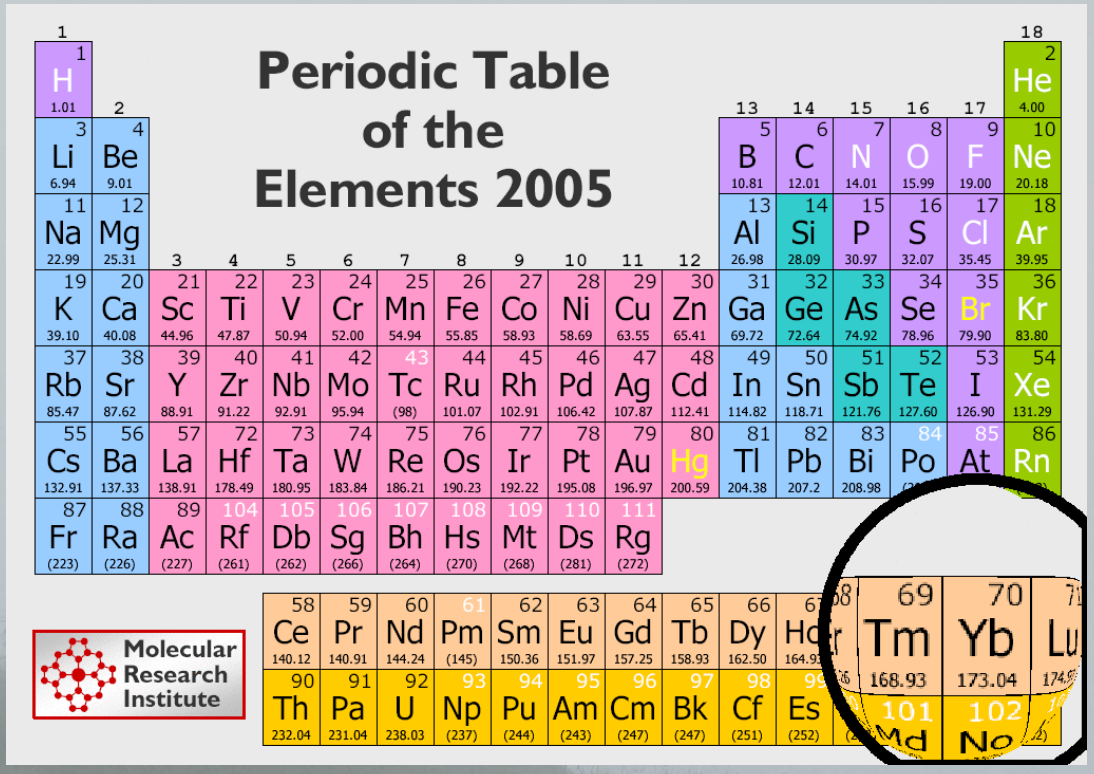

ELNES: fine structure interpretation

Thulium

- Ground state electron configuration: $[Xe].4f^{13}.6s^{2}$
- Shell structure: 2.8.18.31.8.2
- Term symbol: $^{2}F_{7/2}$

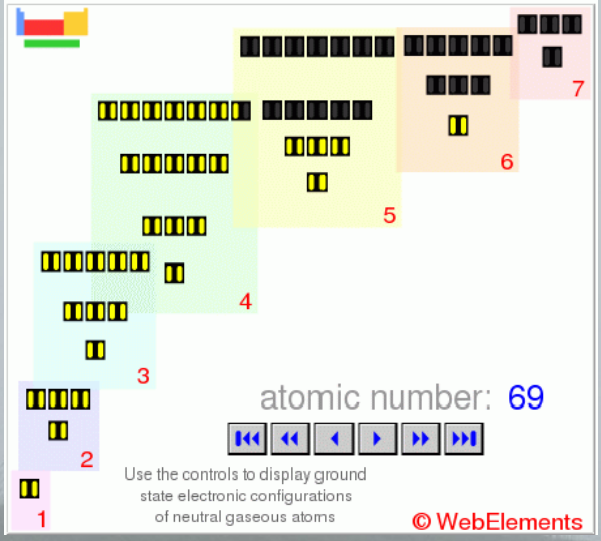

Ytterbium

- Ground state electron configuration: $[Xe].4f^{14}.6s^{2}$
- Shell structure: 2.8.18.32.8.2
- Term symbol: $^{1}S_{0}$

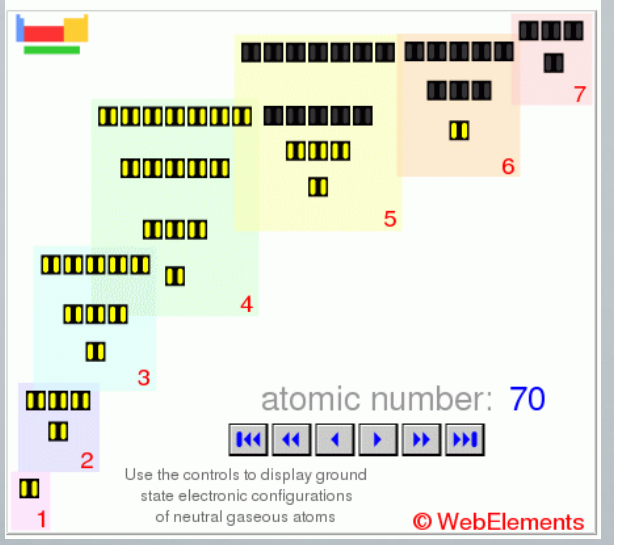

ELNES: fine structure interpretation

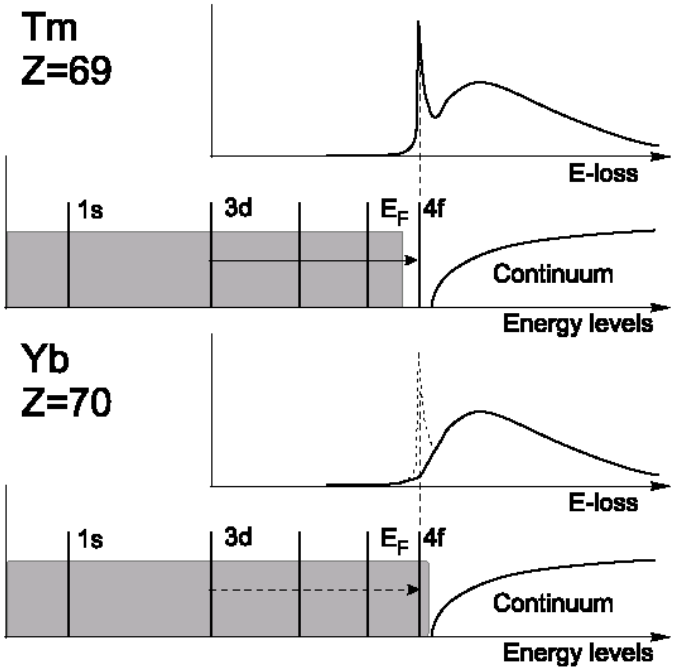

For Yb (Z=70) and higher atomic number, the f-shell is completely filled, and white lines cannot occur.

ELNES: fine structure interpretation

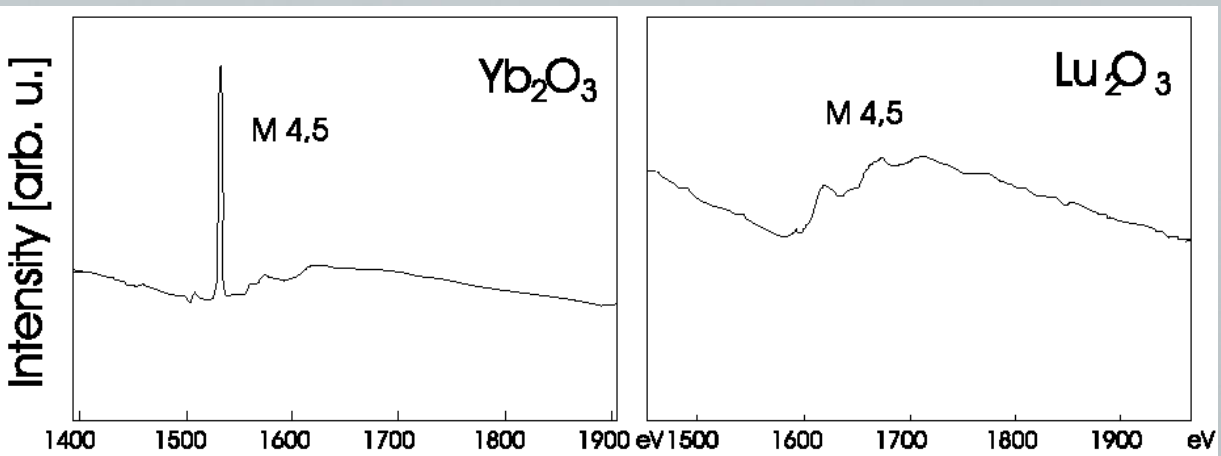

M_{45} edges of Yb and Lu in their oxides, showing the disappearance of white line when the f-subshell is filled.

Using white lines: reduction of NiO

Q. Jeangros, A Hessler-Wyser, Jan van Herle, Cécile Hébert

Anode synthesized as NiO-YSZ

Reduction of NiO to Ni during 1st operation (activation)

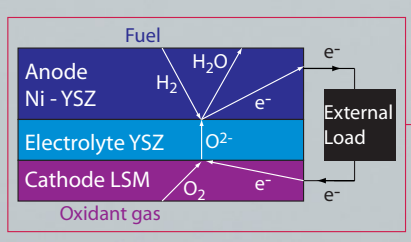

Ni - current conductor & catalyst for H_2 oxidation

YSZ – ionic conductor

Ni structure//chemistry after reduction at 700 °C inside ETEM

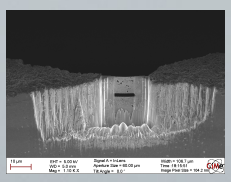

Using white lines: reduction of NiO

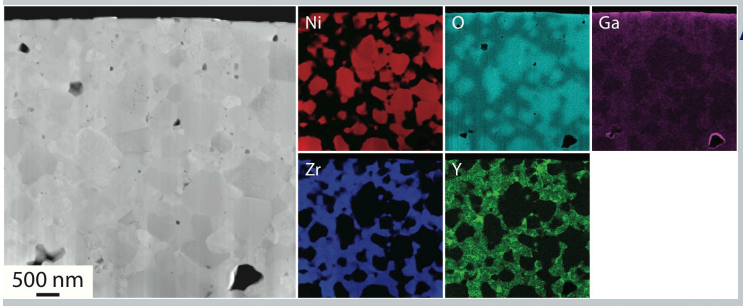

As-sintered NiO-YSZ anode

Phase distribution

Yttria distributed inhomogenously

→ Ionic conduction properties

Gallium due to FIB

< 1.5%at in bulk

> 1.5%at on top of holes

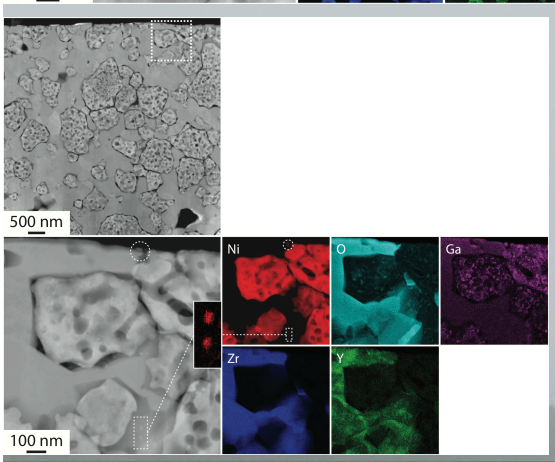

Activated Ni-YSZ anode

Reduction at 700 °C inside ETEM

Porous & inhomogenous Ni structure

Ni nanoparticles

→ Reaction mechanisms

→ $Ni(OH)_2$

Artifact - gallium oxide

Using white lines: reduction of NiO

4 °C/min from 250 to 600 °C

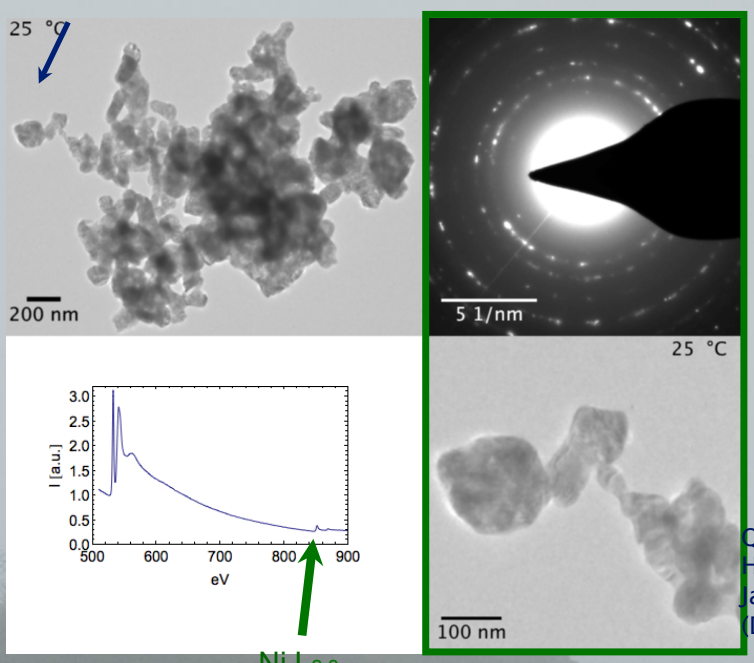

Ni $L_{2,3}$

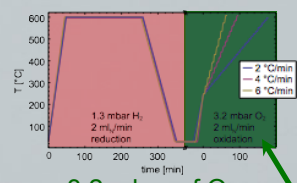

3.2 mbar of O_2

- Some NiO reflections initially
- Small NiO crystallites with random orientations
- Ni to NiO
- Volume expansion
- Internal interface recession

Q. Jeangros, A Hessler-Wyser, Jan van Herle, Cécile Hébert
Jakob Wagner, Rafal Dunin-Borkowski (DTU)

* 1 image, SADP, EELS every 6 minutes

Using white lines: reduction of NiO

Kinetics by EELS

Changes of shape of Ni $L_{2,3}$
→ experimental Ni & NiO references

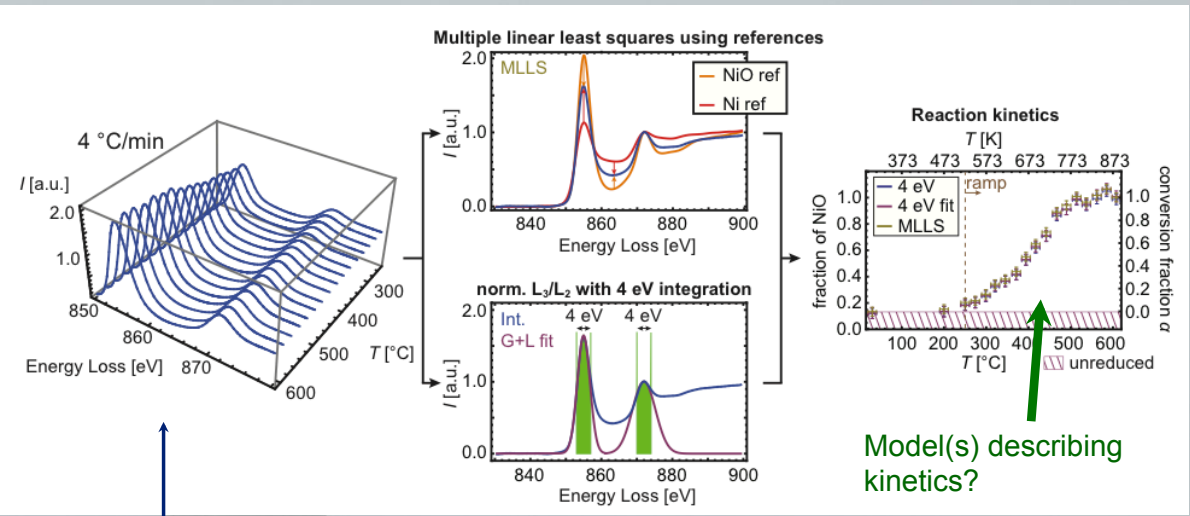

Model(s) describing kinetics?

PCA
Background subtracted
Normalized to 1 at L_2
Energy shift not taken into account (- 0.2 eV)
Convoluted with PSF to get same initial NiO L_3 resolution at 2, 4 & 6 °C/min

$$\beta \cdot \frac{d\alpha}{dT} = A\, e^{-\left(\frac{E_a}{RT}\right)} \cdot f(\alpha)$$

See Jeangros Q et al. (2013), JofMS (48).

Using white lines: reduction of NiO

(Linear) diffusion controls the reaction

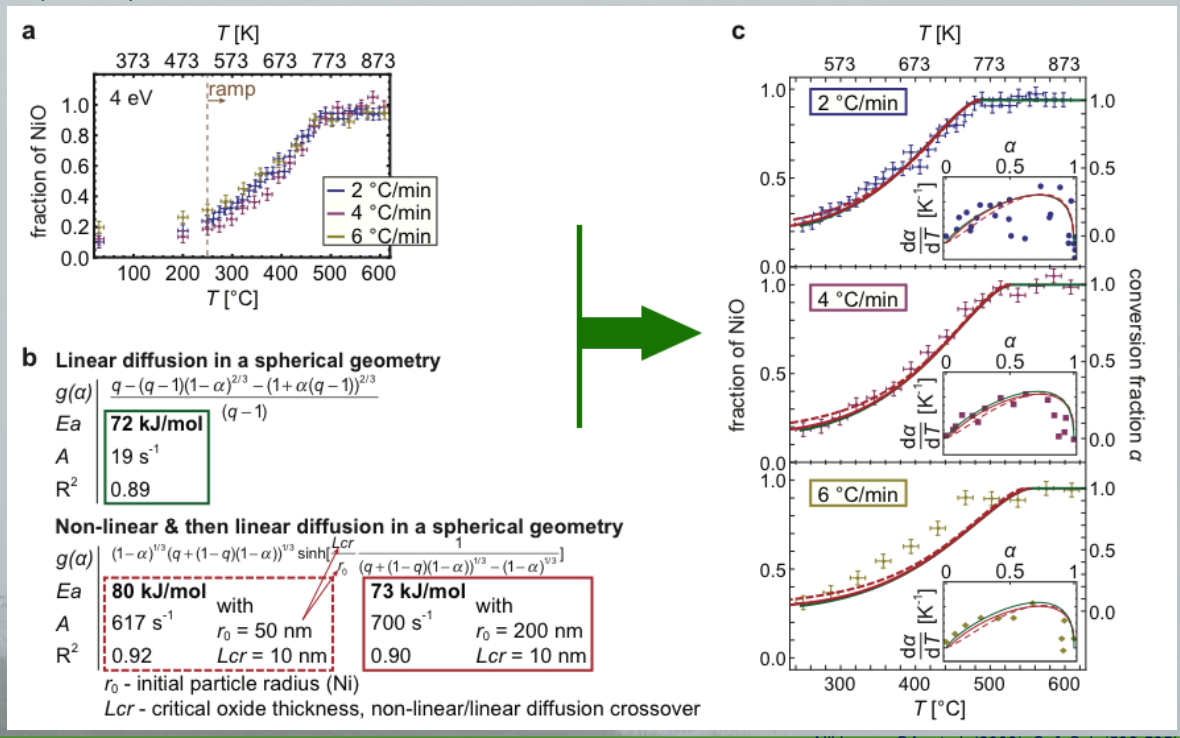

Niklasson GA, et al. (2003), Suf. Sci. (532-535) 324.
Fromhold AT, (1988), J. of Phy. & Chem. of Sol. (49) 1159.

$$S(\vec{q},E) = \sum_F |\langle F|e^{i\vec{q}.\vec{R}}|I\rangle|^2 \delta(E_I - E_F + E)$$

Final state: ??

Initial state: Core state

Next step: take crystal into account for |F>

Ab-initio calculations. One large family of methods: density functional theory

ELNES: fine structure calculation

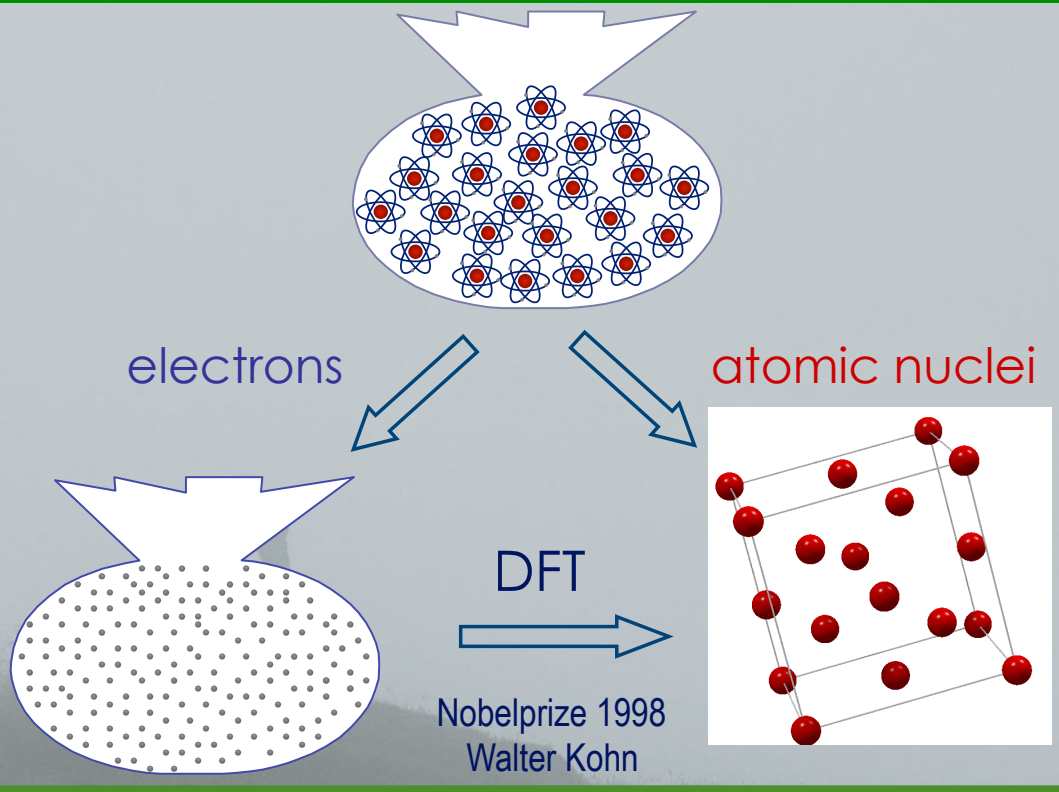

ELNES: fine structure

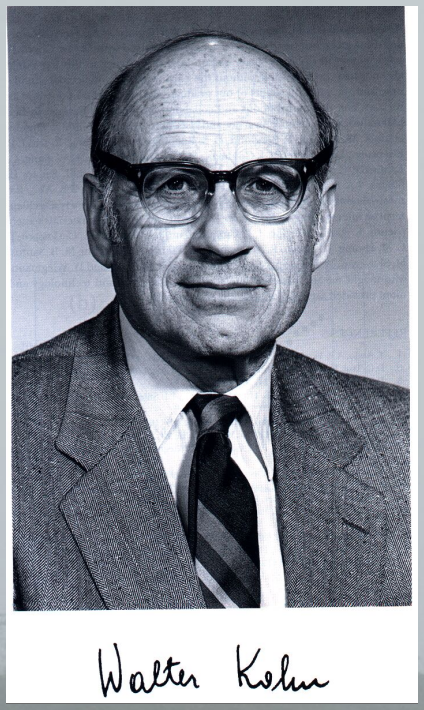

Walter Kohn
Nobel prize
laureate 1998
chemistry

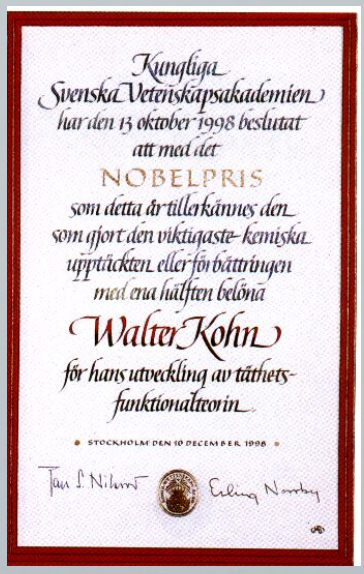

WIEN2k

Full potential (FP)
Muffin-tin (MT)
atomic sphere (ASA)
pseudopotential (PP)

Form of potential

Relativistic treatment

fully-relativistic
semi-relativistic
non relativistic

exchange and correlation "potential"

Local density approximation (LDA)
Generalized gradient approximation (GGA)
Beyond LDA: e.g. LDA+U

$$\left[-\frac{1}{2}\nabla^2 + V(r)\right]\varphi_i^k = \varepsilon_i^k \varphi_i^k$$

Kohn-Sham equations

$$V_{ext}(\vec{r}) + V_C(\rho(\vec{r})) + V_{xc}(\rho(\vec{r}))$$

non periodic
(cluster)
periodic
(unit cell)

Representation of solid

Spin polarized
non spin polarized

Treatment of spin

Basis functions

plane waves : PW
augmented plane waves : APW
linearized "APWs"
analytic functions (e.g. Hankel)
atomic orbitals. e.g. Slater (STO), Gaussians (GTO)
numerical

courtesy K.H. Schwarz

ELNES: fine structure

Electron density
-> Wave functions
-> Density of states
-> unoccupied density of states

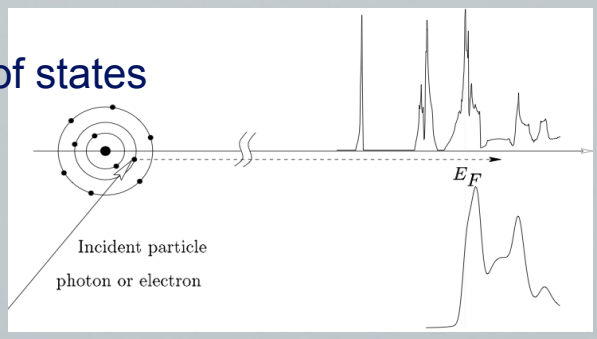

EELS spectrum with fine structures!

Compare with experiment

ELNES: fine structure

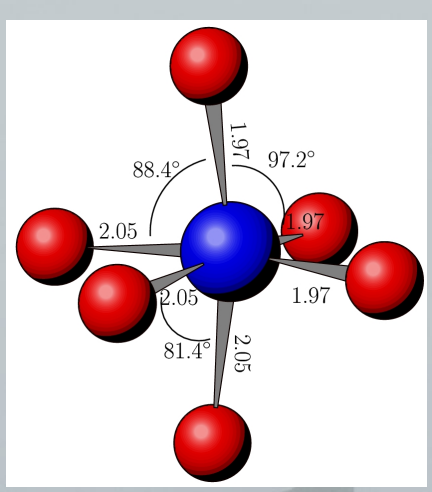

V_2O_5

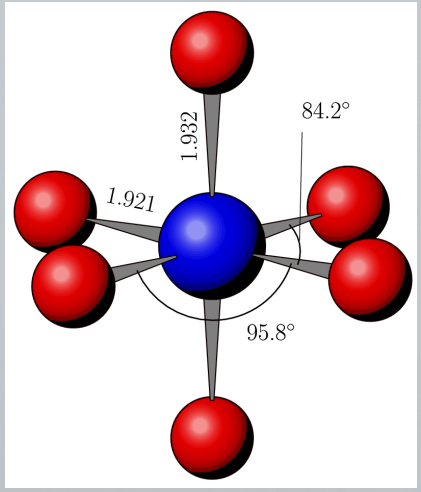

VO_2

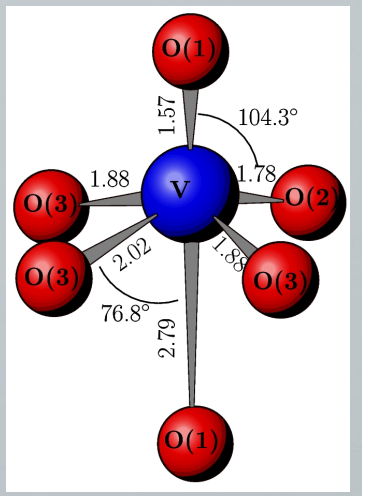

V_2O_3

C. Hébert, et al.
Eur.Phys.J B 28, 407 (2002)

ELNES: fine structure

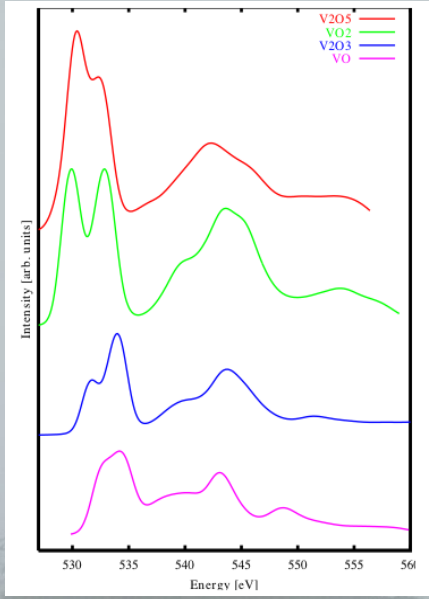

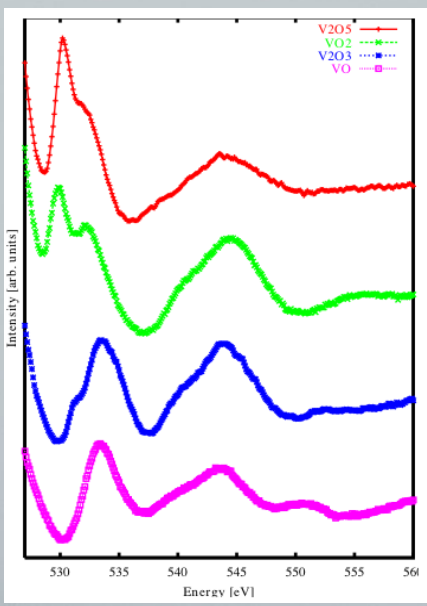

C. Hébert, et al.
Eur.Phys.J B 28, 407 (2002)

Core Loss: theory

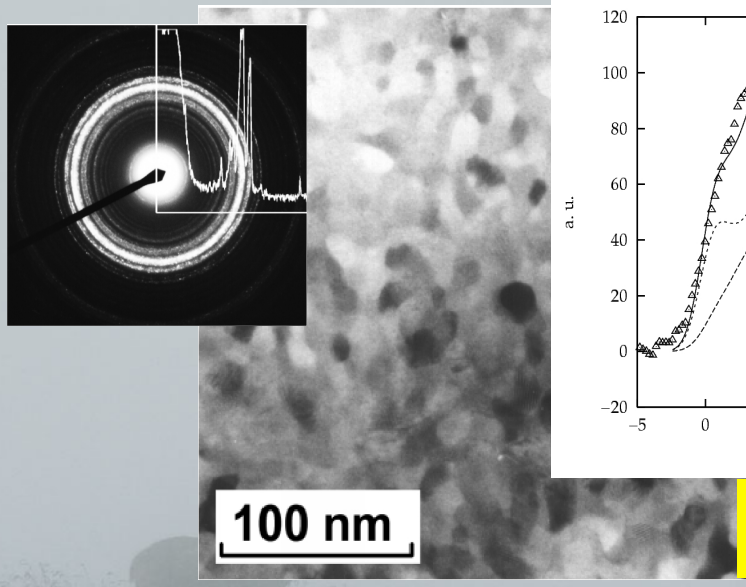

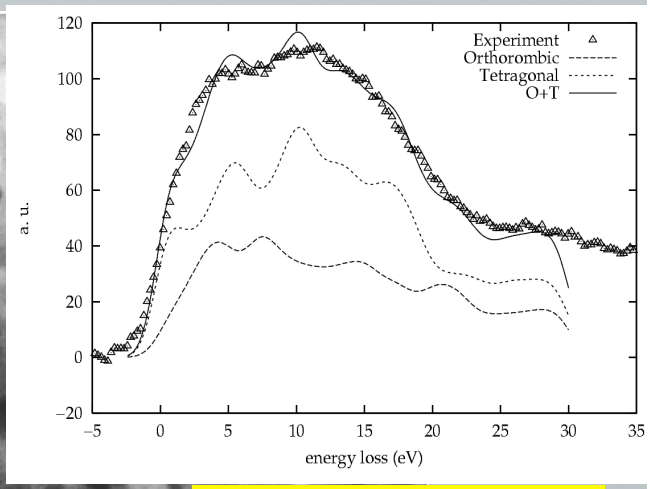

Distinction of two BFe3 phases by ELNES. 70% tetragonal from linear least sq. fit

C. Hébert & al. EPJ- Applied Physics, 9:147 (2000)

Introduction

$$S(\vec{q},E) = \sum_F |\langle F|e^{i\vec{q}.\vec{R}}|I\rangle|^2 \delta(E_I - E_F + E)$$

Final state: ??

Initial state: Core state

Further : consider real electron wave in the crystal (instead of plane wave) e.g. P. Schattschneider, Oxley & Pantelides

New developments

PRL 109, 246101 (2012) PHYSICAL REVIEW LETTERS week ending 14 DECEMBER 2012

Simulation of Spatially Resolved Electron Energy Loss Near-Edge Structure for Scanning Transmission Electron Microscopy

M. P. Prange,[1,2,*] M. P. Oxley,[1,2,†] M. Varela,[2] S. J. Pennycook,[2,1] and S. T. Pantelides[1,2,3]

[1]*Department of Physics and Astronomy, Vanderbilt University, Nashville, Tennessee 37235, USA*
[2]*Materials Science and Technology Division, Oak Ridge National Laboratory, Oak Ridge, Tennessee 37831, USA*
[3]*Department of Electrical Engineering and Computer Science, Vanderbilt University, Nashville, Tennessee 37235, USA*
(Received 29 August 2012; revised manuscript received 9 November 2012; published 12 December 2012)

Aberration-corrected scanning transmission electron microscopy yields probe-position-dependent energy-loss near-edge structure (ELNES) measurements, potentially providing spatial mapping of the underlying electronic states. ELNES calculations, however, typically describe excitations by a plane wave traveling in vacuum, neglecting the interaction of the electron probe with the local electronic environment as it propagates through the specimen. Here, we report a methodology that combines a full electronic-structure calculation with propagation of a focused beam in a thin film. The results demonstrate that only a detailed calculation using this approach can provide quantitative agreement with observed variations in probe-position-dependent ELNES.

New developments

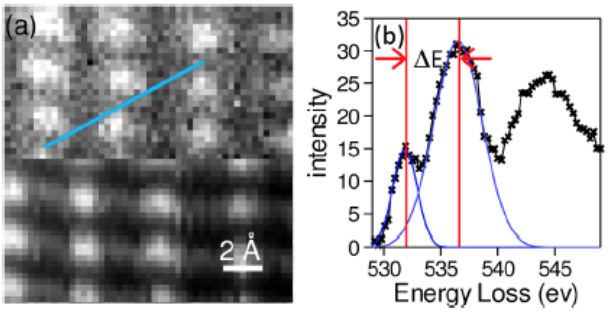

FIG. 2 (color online). (a) Integrated experimental O K-shell intensity (top) and simultaneously acquired ADF signal (bottom). (b) A typical spectrum showing schematically the ΔE measurement. The line scan indicated on (a) is the same as that used in Fig. 4.

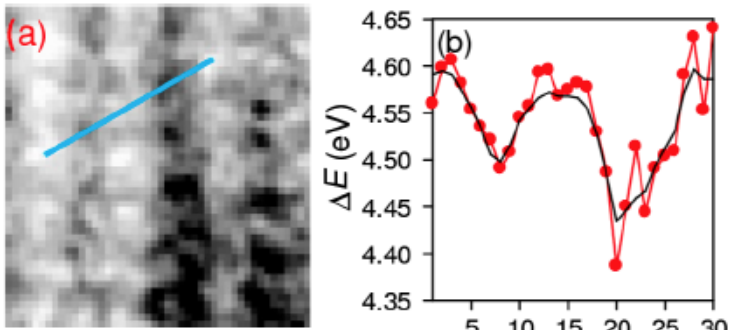

New developments

Microsc. Microanal. 20, 784–797, 2014
doi:10.1017/S1431927614000610

Oxley & al. Simulation of Probe Position-Dependent Electron Energy-Loss Fine Structure

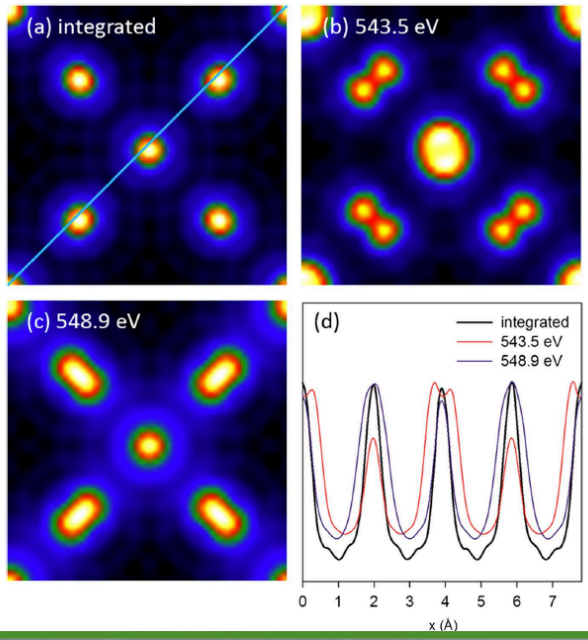

Oxygen K-shell ionization scattering potentials in STO for
(a) the energy integrated potential,
(b) (**b**) for **E**loss = 543.5 eV
and (c) **E**loss = 548.9 eV,

(**d**) normalized diagonal intensity line scans as indicated by the cyan line shown on (**a**).

An energy broadening of 0.35 eV has been applied in all cases.

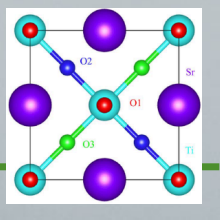

Outline

- Introduction: EELS in the TEM
- Core losses
- Low losses
- Even lower losses
- Conclusion

Introduction

Low losses

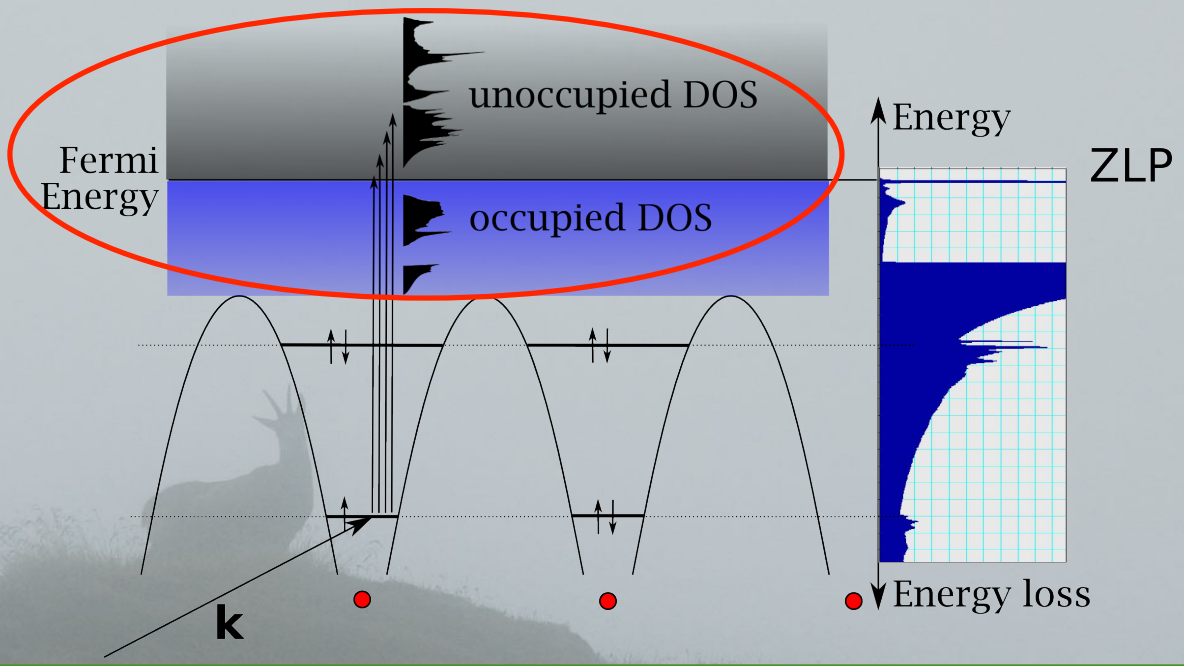

Low Loss

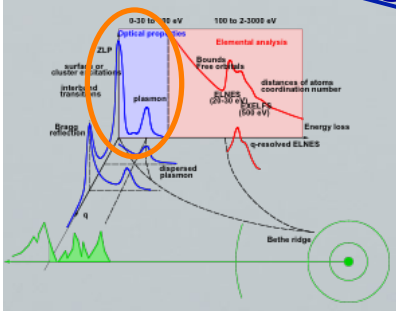

Visible light

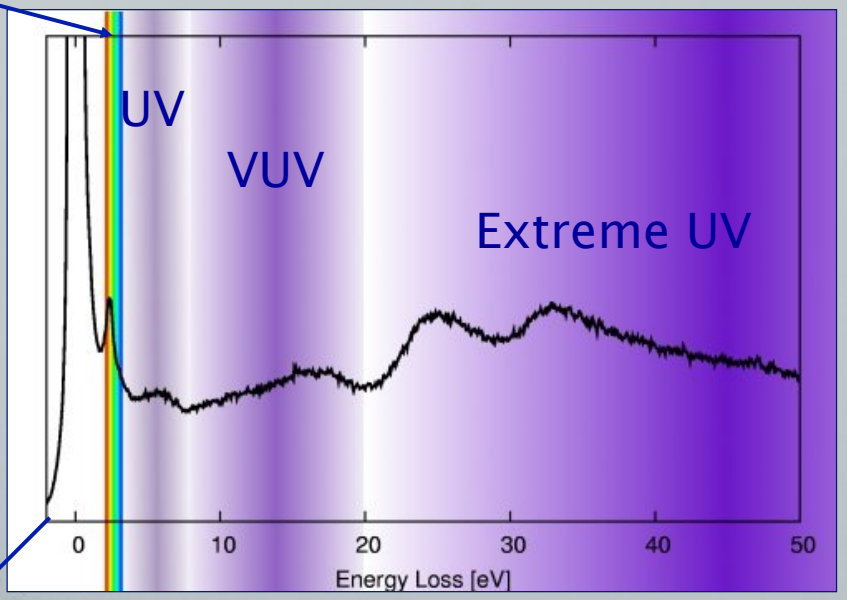

Plasmons (collective oscilations)

Interband transitions

Scattering angle (momentum transfer)

Low Loss

SSD and loss function

$$S(E) = \left[\frac{e^2}{\pi\hbar v}\right]^2 \cdot D \cdot \Im\left[\frac{-1}{\varepsilon(E)}\right] \cdot \ln\left[1 + \left(\frac{\beta}{\theta_E}\right)^2\right]$$

single scattering distribution

Sample thickness

Loss function

Angular scattering distribution

Low Loss: KKA

From the experiment to the loss function: theory

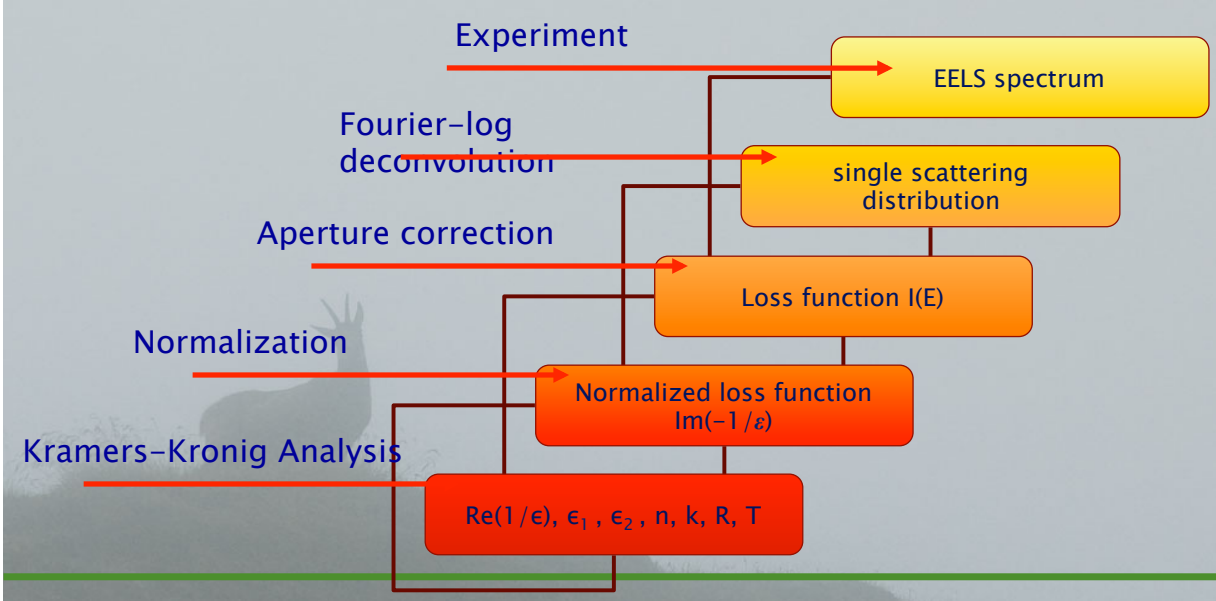

Low Loss: the Kröger equation

The relation between the double differential cross section and the loss function is a „little bit“ more complicated

$$\frac{\partial P(\omega,\mathbf{k}_\perp)}{\partial\omega\partial^2 k_\perp} = \frac{e^2}{\pi^2\hbar v^2}\cdot\Im\left[\frac{\mu^2}{\epsilon\phi^2}\cdot D\right.$$

Volume term

$$-\frac{2k_\perp^2(\epsilon-\epsilon_0)^2}{\phi_0^4\phi^4}\cdot\left\{\frac{\phi_{01}^4}{\epsilon\epsilon_0}\left(\frac{sin^2(\frac{\omega D}{2v})}{L^+}+\frac{cos^2(\frac{\omega D}{2v})}{L^-}\right)\right.$$

$$+\beta^2\cdot\frac{\lambda_0\omega\phi_{01}^2}{\epsilon_0 v}\cdot\left(\frac{1}{L^+}-\frac{1}{L^-}\right)\cdot sin\left(\frac{\omega D}{v}\right)$$

$$\left.\left.-\beta^4\cdot\frac{\omega^2}{v^2}\cdot\lambda_0\lambda\left(\frac{cos^2(\frac{\omega D}{2v})tanh(\lambda D/2)}{L^+}+\frac{sin^2(\frac{\omega D}{2v})coth(\lambda D/2)}{L^-}\right)\right\}\right]$$

Following abbreviations were used:

$$\lambda=\sqrt{k_\perp^2-\frac{\epsilon\omega^2}{c^2}},\quad \lambda_0=\sqrt{k_\perp^2-\frac{\epsilon_0\omega^2}{c^2}}$$

$$L^+=\lambda_0\epsilon+\lambda\epsilon_0 tanh(\lambda D/2),\quad L^-=\lambda_0\epsilon+\lambda\epsilon_0 coth(\lambda D/2)$$

$$\beta^2=\frac{v^2}{c^2},\quad \phi_{01}^2=k_\perp^2+\frac{\omega^2}{v^2}-(\epsilon+\epsilon_0)\frac{\omega^2}{c^2}$$

$$\phi^2=\lambda^2+\frac{\omega^2}{v^2},\quad \phi_0^2=\lambda_0^2+\frac{\omega^2}{v^2}$$

$$\mu^2=1-\epsilon\beta^2,\quad \mu_0^2=1-\epsilon_0\beta^2$$

Z. Phys. 216 (1968), 115-135

Low Loss

Relativistic effects in semiconductors - Bulk

A lower TEM-acceleration voltage allows higher n-materials!

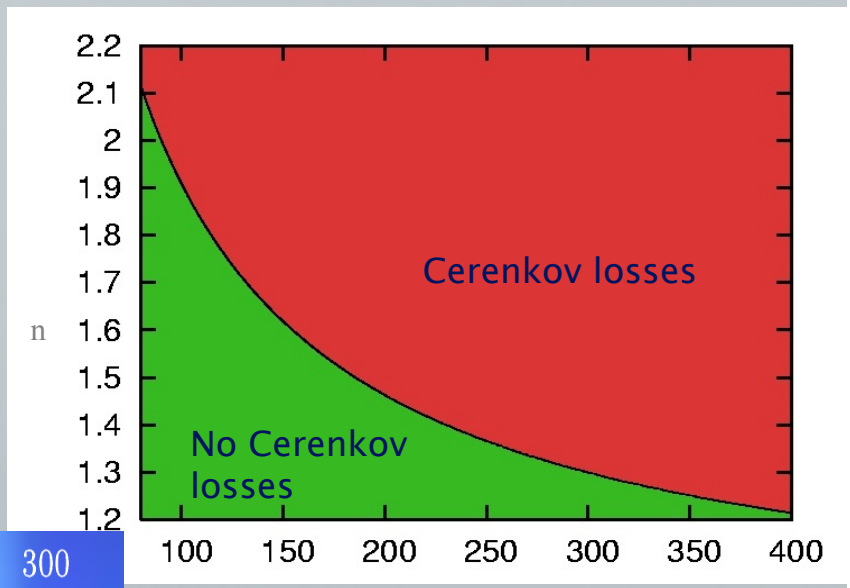

kV	100	200	300
n	1.8242	1.4381	1.2878
ϵ_1	3.3278	2.0683	1.6584

Low Loss: some solutions

Decrease TEM voltage (SiN_x:H)

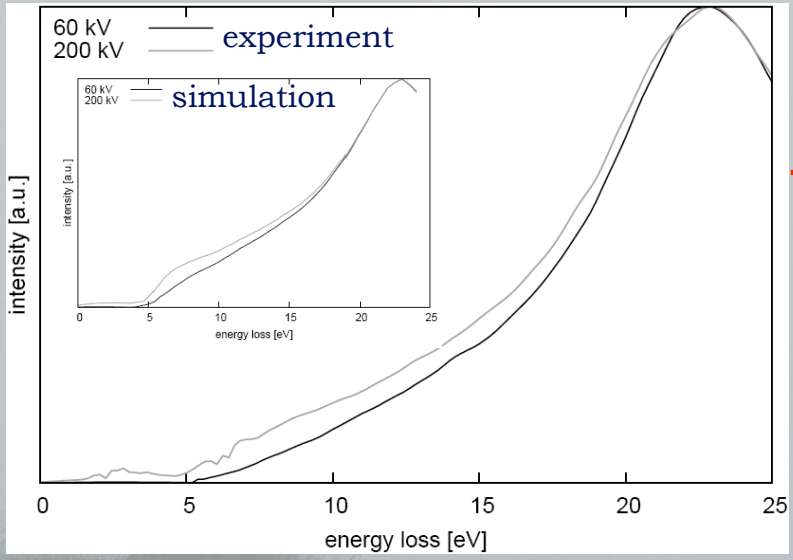

KKA – refractive index

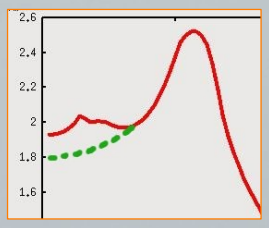

0 eV 10

M. Stöger-Pollach, UM 107, (2007) p. 1178-85

Low Loss: some solutions

difference method (Si)

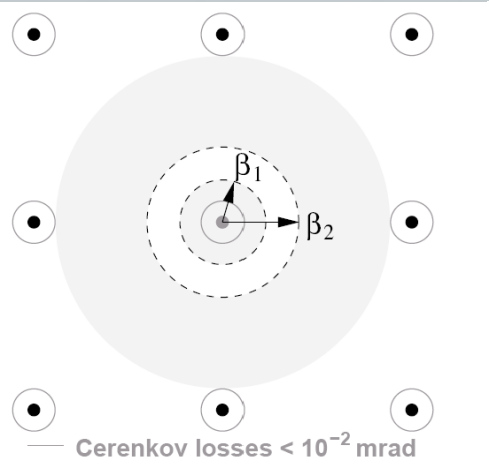

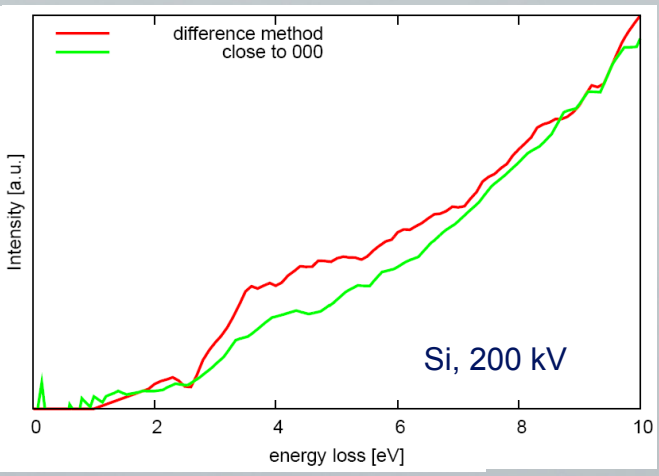

M. Stöger-Pollach, UM 107, (2007) p. 1178-85

Low Loss

Comparison with theory ?

$$S(E) = \left[\frac{e^2}{\pi\hbar v}\right]^2 \cdot D \, \Im\left[\frac{-1}{\varepsilon(E)}\right] \cdot \ln\left[1 + \left(\frac{\beta}{\theta_E}\right)^2\right]$$

Alkauskas & al..

PHYSICAL REVIEW B 88, 195124 (2013)

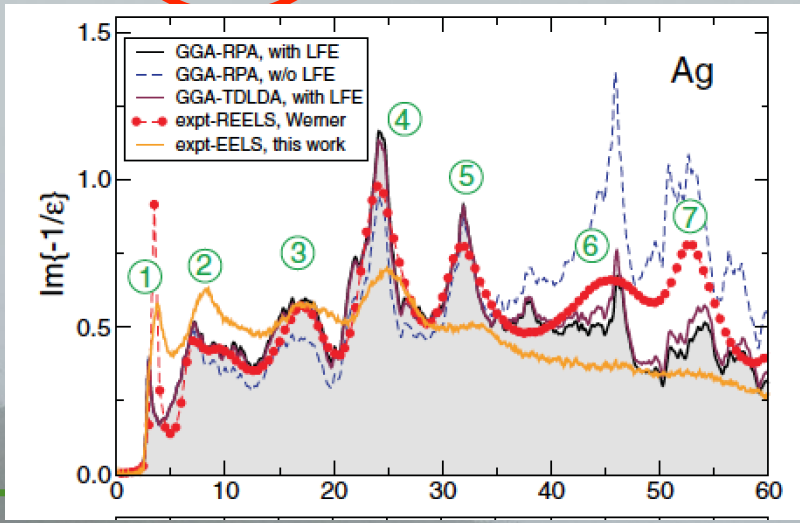

Low Loss

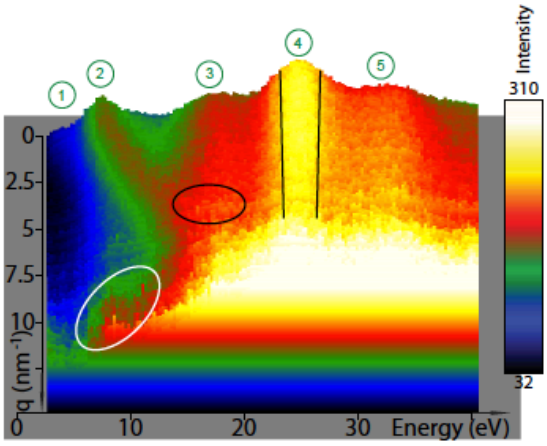

Experimental data with $q \rightarrow$[100] and $q \rightarrow$[110] contribution

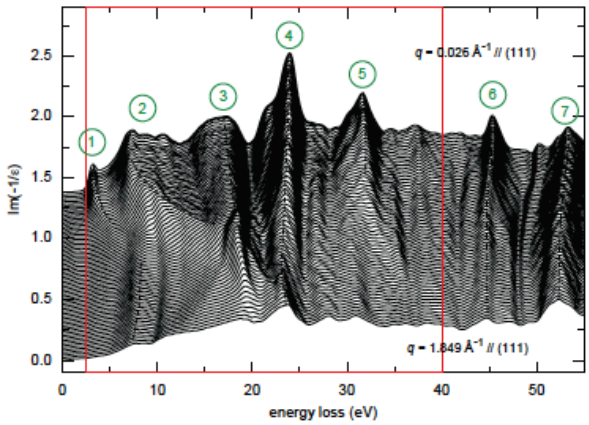

Alkauskas *et al.*, Ultramicroscopy **110**(8), 1081-1086 (2010)

Theory: calculation of $\Im\left[\frac{-1}{\varepsilon}\right]$ from the band structure via RPA

Outline

- Introduction: EELS in the TEM
- Core losses
- Low losses
- Even lower losses
- Conclusion

Introduction

Excitation process

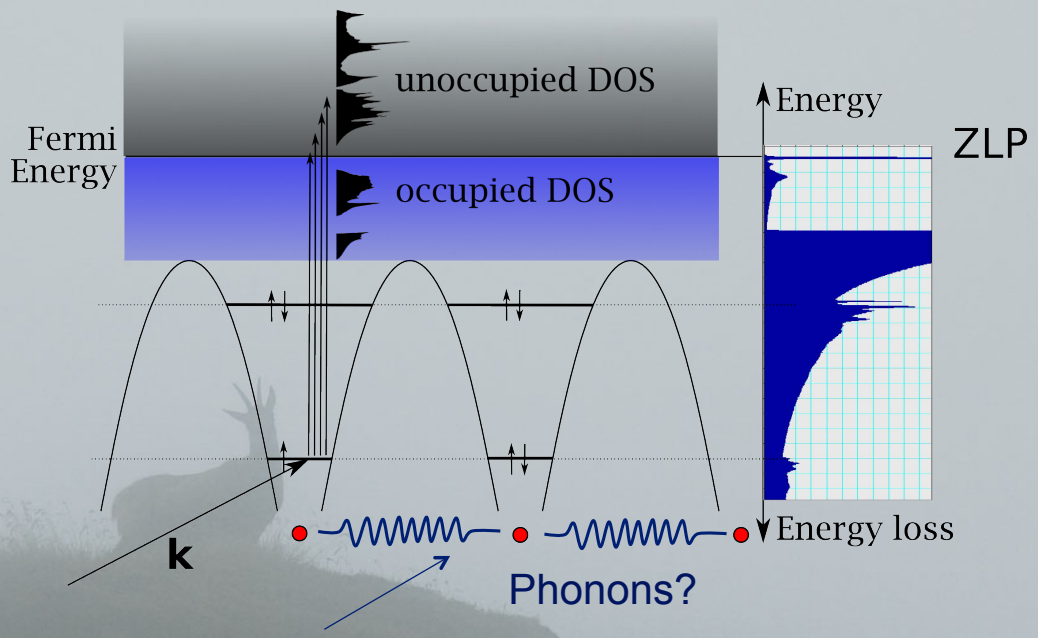

High Energy Resn Monochrmtd EELS-STEM (HERMES)

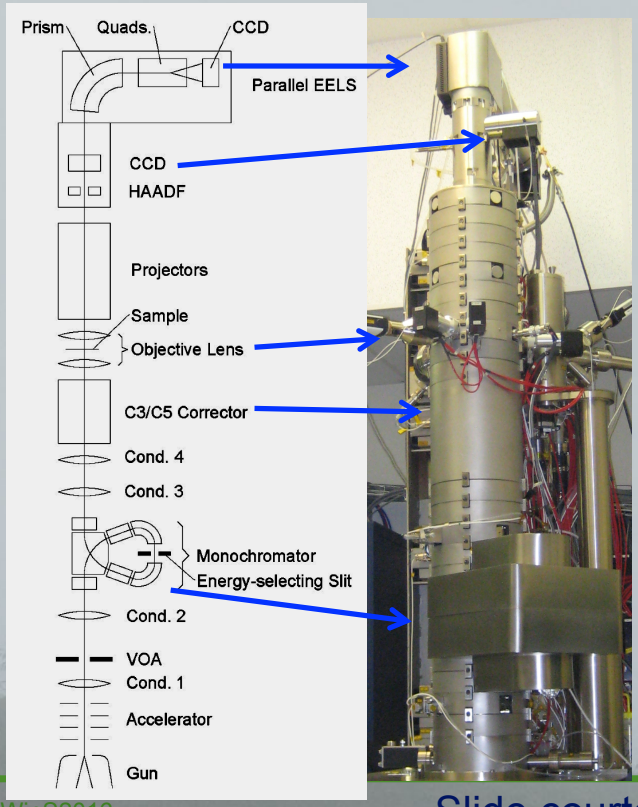

microscope height = 3.2 m

The first monochromator system built was designed for 40-100 keV operation. However, extension to 200 keV will be very straight-forward.

First system delivered to ASU (Ray Carpenter, PI) in January 2013.

Subsequent systems: Rutgers U. (Sept 2013), Daresbury Super-STEM (planned), CNRS Orsay (200 kV, planned).

Slide courtesy: O. Krivanek

30x improvement of EELS energy resolution!

Low Loss EELS Spectroscopy with a Monochromated Cold FEG NION D-STEM

R. W. Carpenter[1,2], H. Xie[3], J. Mardinly[1], T. Aoki[1], S. Lehner[2], Y. O. Wei[4], M. Vahidi[3], N. Newman[3], F. A. Ponce[4]
1. LeRoy Eyring Center for Solid State Science, Arizona State U, Tempe, AZ 85287, USA; 2. Dept. of Chemistry and Biochemistry, Arizona State U, Tempe, AZ 85287, USA; 3. School for Engr. of Matter, Transport, and Energy, Arizona State U, Tempe, AZ 85287 USA; 4. Dept. of Physics, Arizona State U, Tempe, AZ 85287, USA

Fig. 4. Superimposed typical zero loss peaks from the monochromated NION (red) and the STEM corrected Schottky FEG ARM at ASU. Normalized to the same total peak intensity. Note the reduced beam tails for the monochromated NION.

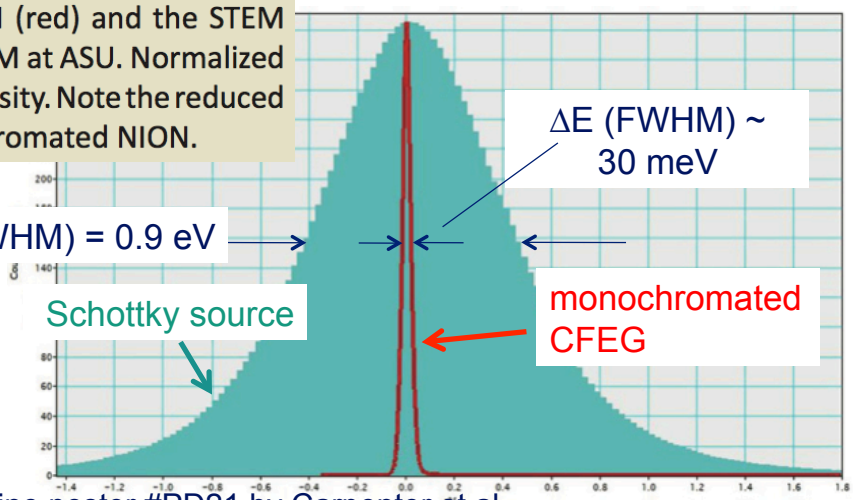

M&M 2013 post-deadline poster #PD21 by Carpenter et al.

Slide courtesy: O. Krivanek

High energy resolution ZLP acquired with HERMES

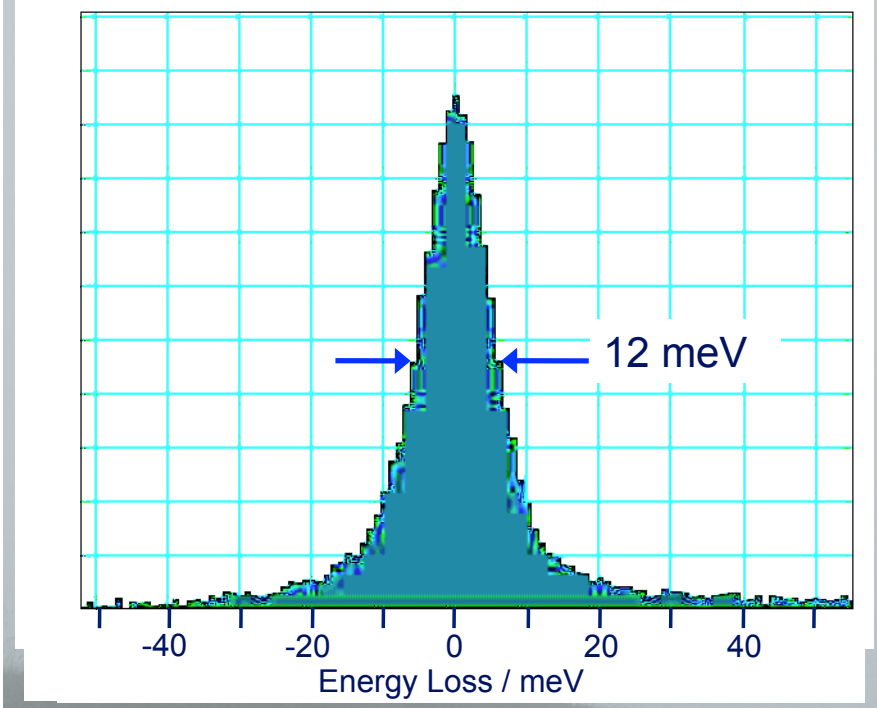

Spectrum of the zero loss peak acquired in 250 ms.

60 keV, Nion HERMES

Extra-stable EEL spectrometer, Rutgers U.

Courtesy Niklas Dellby and Phil Batson

Slide courtesy: O. Krivanek

Phonon mapping

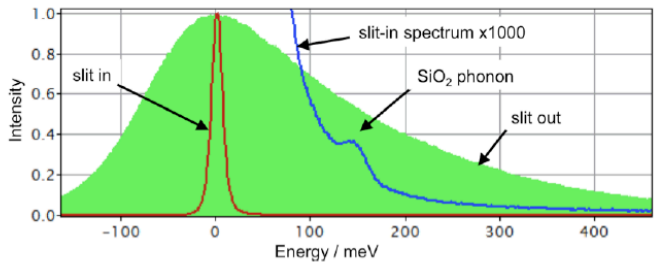

Figure 1. EEL spectra recorded with the monochromator slit out (green) and in (red and blue).

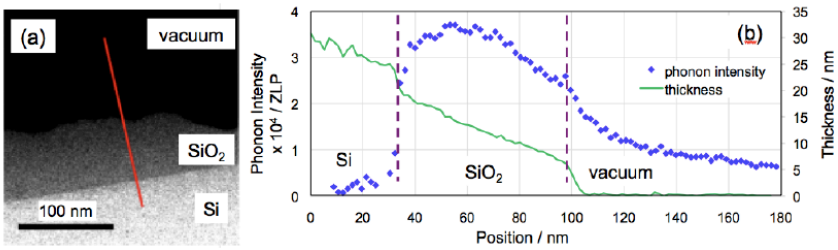

Figure 2. Variation of the phonon signal intensity in a line profile taken from Si via SiO_2 into vacuum. 60 keV, 10 pA probe current. (a) HAADF image showing profile location. (b) Profile showing the phonon intensity and the sample thickness. Sample courtesy Dr. John Bruley, IBM.

We have also been able to improve the rate of the decay of the zero loss peak (ZLP) such that tail intensities of <4x10-4 of the ZLP maximum have been recorded at energy losses as small as 100 meV.

Phonon mapping with monochromated STEM EELS

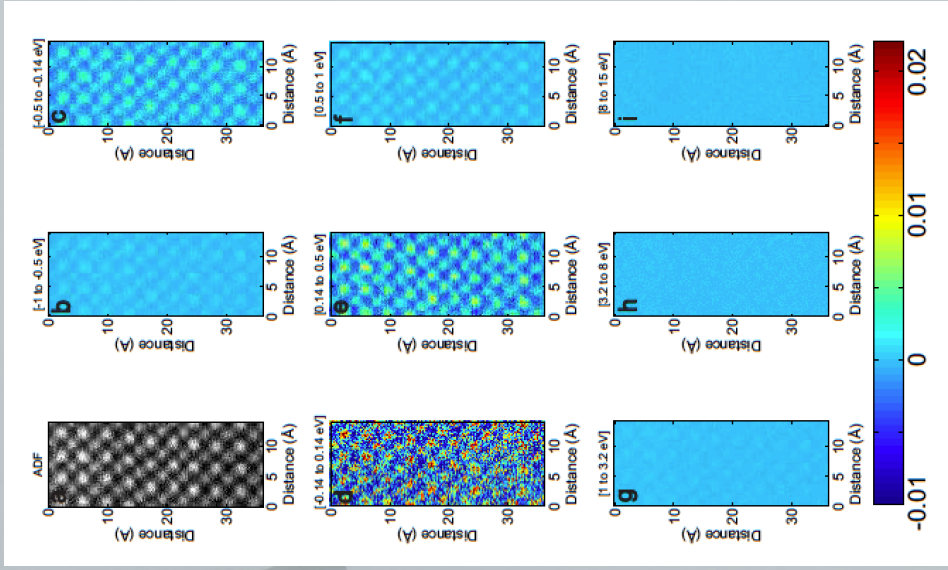

Figure 4: HAADF image and its corresponding selected *subtracted* spectrum-image integrated over different energy ranges of [-1.0 to -0.5 eV]; [-0.5 eV to -0.14 eV]; [-0.14 to 0.14 eV]; [0.14 to 0.5 eV]; [1.0 to 3.2 eV]; [3.2 to 8.0 eV] and [8.0 to 15 eV]. Images are plotted using the same color scale.

Egoeavil & al.
Ultramicroscopy
Volume 147, 2014, Pages 1–7

Outline

- Introduction: EELS in the TEM
- Core losses
- Low losses
- Even lower losses
- Conclusion

Challenges:

- High spatial **and** high energy resolution can only be achieved with a **Convergent probe** !
- Cs corrected STEM. Several 10 of mradians convergence. (1st diffraction @10).
- The incoming electron is everything but a plane wave…
- Geometry, thickness, orientation of the specimen matters

Conclusion

- Huge amount of information in ELNES
- No need for super-high energy resolution
- Already simple interpretation give lot of information
- Many ways to calculate ELNES
- Still active field of development

TEM, EELS and simulation

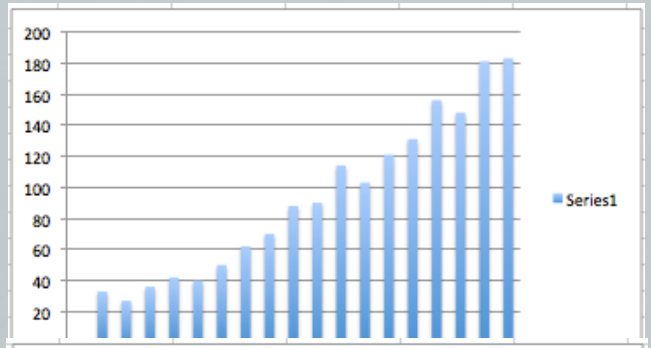

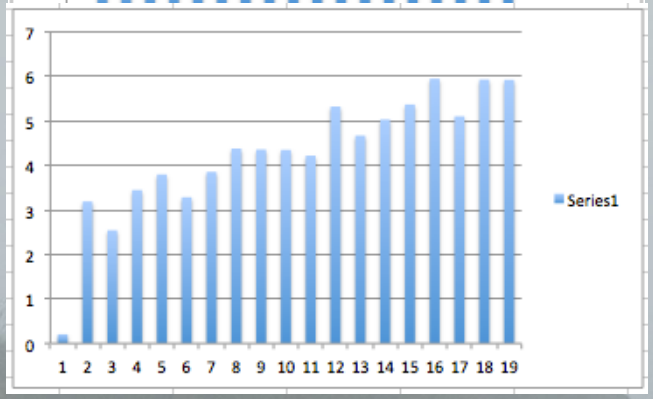

TEM and
EELS and
DFT or Ab Initio
Per year
From 1995 to 2013

Same as previous
*1000 / TEM